

UCLA

UCLA Electronic Theses and Dissertations

Title

Using a multi-satellite synergy algorithm and a chemical transport model to assess the environmental impact of a disaster: The case of the wildfires of 2020.

Permalink

<https://escholarship.org/uc/item/9q10x91j>

Author

Neyra Nazarrett, Oscar Alejandro

Publication Date

2023

Peer reviewed|Thesis/dissertation

UNIVERSITY OF CALIFORNIA

Los Angeles

Using a multi-satellite synergy algorithm and
a chemical transport model to assess the environmental impact of a disaster:

The case of the wildfires of 2020.

A dissertation submitted in partial satisfaction of
the requirements for the degree
Doctor of Environmental Science and Engineering

by

Oscar Alejandro Neyra Nazarrett

2023

© Copyright by

Oscar Alejandro Neyra Nazarrett

2023

ABSTRACT OF THE DISSERTATION

Using a multi-satellite synergy algorithm and
a chemical transport model to assess the environmental impact of a disaster:
The case of the wildfires of 2020.

by

Oscar Alejandro Neyra Nazarrett

Doctor of Environmental Science and Engineering

University of California, Los Angeles, 2023

Professor Pablo Saide Peralta, Co-Chair

Professor Miriam Elizabeth Marlier, Co-Chair

This dissertation employs a multi-satellite synergy algorithm and a chemical transport model to investigate atmospheric composition changes and public health impacts resulting from the 2020 wildfires in the Western United States. The study synergizes data from the CrIS and TROPOMI satellite instruments to analyze carbon monoxide (CO) and evaluates how these two instruments sensed CO separately and in synergy. Results indicate significantly higher daily average CO columns in the Western U.S. compared to the Central and Eastern U.S., with TROPOMI revealing higher values near fire sources, suggesting stronger contributions from close-to-surface concentrations. Validation against ground-based TCCON and NDACC's FTIR CO column estimates demonstrated Normalized Mean Error of less than 24% for CrIS and 32% for

TROPOMI. The synergy between TROPOMI and CrIS CO columns was evaluated by assessing the elevated smoke plume on September 15, 2020, against a balloon-borne retrieval from AirCore. It was found that even when deviations were present in CrIS's predicted profile, consistency between TROPOMI and CrIS CO columns was maintained for lofted plumes. Overall, this analysis shows that CrIS and TROPOMI provide complementary information on CO, enhancing the understanding of CO distribution during the wildfires.

The dissertation then focuses on a detailed study of fire-specific PM_{2.5} emissions, employing the GEOS-Chem chemical transport model. This section reveals that the 2020 wildfires resulted in an unprecedented emission of 328 million tons PM_{2.5} across the Western U.S., far exceeding the total emissions of the previous three years. It highlights that California alone was responsible for 18% of the six-year total PM_{2.5} emissions in 2020. The study revealed that certain locations in the Western United States experienced prolonged periods of hazardous air quality conditions that exceeded the EPA's 24-hour limits for more than 40 days. In total, there were 492 million person-days of exposure to poor air quality in the Western U.S. in 2020. This study emphasizes the importance of distinguishing between emissions from fire-specific smoke and smoke from multiple sources due to the higher toxicity of wildfire smoke.

The aim of this research is to highlight the importance of understanding the impact of wildfires on the environment and populations, especially considering their increasing frequency and severity.

The dissertation of Oscar Alejandro Neyra Nazarrett is approved.

Thomas Welch Gillespie

Kevin W Bowman

Miriam Elizabeth Marlier, Committee Co-Chair

Pablo Saide Peralta, Committee Co-Chair

University of California, Los Angeles

2023

DEDICATION

To my mother, who taught me the value of discipline, working to finish college and raising me at the same time. Every night I worked on this dissertation I thought of her and the sound of her mechanic typewriter. To my father, for giving me character to make of every adversity an opportunity, thank you for being my best friend. To my sister, for her infinite love and for teaching me that it is the unlikely what governs the universe. To my uncles for being my second parents and for teaching to rise to every occasion. To my cousins, who gave me some of the most important lessons in my life. Thanks for teaching me not to be afraid of any risk. There are some things that can only be learned on the streets. And very especially this dissertation is dedicated to Veronica, the love of my life.

TABLE OF CONTENTS

ABSTRACT OF THE DISSERTATION	ii
DEDICATION	v
TABLE OF CONTENTS	vi
LIST OF TABLES	ix
LIST OF FIGURES	x
ACKNOWLEDGEMENTS.....	xii
VITA	xiii
Chapter 1 Introduction.....	1
Chapter 2 A multi-satellite synergy algorithm to assess and validate CO measurements during the wildfires of 2020	8
2.1 Abstract	8
2.2 Introduction	10
2.2.1 Use of satellite retrievals to study CO	11
2.2.2 Previous work validating CrIS and TROPOMI CO retrievals.....	13
2.2.3 Satellite synergies.	15
2.3 Data and Method	16
2.3.1 Satellite CO retrievals	16
2.3.2 Reference Data.....	18
2.3.3 Satellite synergy	22
2.3.4 FTIR Co-location.....	23
2.3.5 Processing of Aircore data	25
2.4 Results and Discussion.....	26

2.4.1	Synergy Evaluation	26
2.4.2	Data Validation.....	30
2.5	Conclusions and Future Directions	35
Chapter 3	Contributions of 2020 wildfires to western U.S. air pollution.....	39
3.1	Abstract	39
3.2	Introduction	41
3.3	Data and Methods.....	46
3.3.1	GEOS-Chem Configuration.....	46
3.3.2	Observational Datasets Used for Model Validation.....	48
3.3.3	Population-Level Exposure.....	50
3.4	Results	50
3.4.1	Fire emissions	50
3.4.2	GEOS-Chem Simulation Results.....	52
3.4.3	GEOS-Chem Validation.....	53
3.4.4	Population exposure.....	58
3.5	Discussion	60
3.5.1	Summary of Results.....	60
3.5.2	Limitations	62
3.5.3	Implications and future work.....	63
3.6	Conclusions	64
4	Overarching conclusion	66
Appendices.....		68
Appendix A.....		68

Appendix B.....	70
References.....	78

LIST OF TABLES

Table 1: Overview of the Satellite CO products assessed.....	16
Table 2: Ground based Fourier transform spectrometers (FTSs) and corresponding network.	20
Table 3: Key statistics of the co-located satellite retrievals that correspond to each of the ground based measurements.....	33
Table 4: Comparison of smoothed CO column for the aircore profile compare to satellite columns.....	35
Table 5: Annual GFAS fire emissions statewide from 2015-2020 (Teragrams).	51
Table 6: Persons days exposed.....	59

LIST OF FIGURES

Figure 1: Comparison of CrIS high-resolution data (0.25 degrees) versus homogenized version of TROPOMI for the three regions of interest	27
Figure 2: Timeseries Comparison of 2020 Fire Season Daily Mean Total Columns Derived from Satellite Retrievals across Western, Central, and Eastern U.S. Western region, juxtaposed with Fire Radiative Power (FRP) Measurements in the Western U.S."	29
Figure 3: Timeseries validation of 2020 daily average CO column satellite measurements co-located with FTIR ground-based measurements in Boulder, Pasadena, Lamont, and Park Falls. 32	
Figure 4: Comparing vertical profiles of CrIS co-located with Smoothed Aircore VMR profiles.	35
Figure 5: Annual average emissions of GFAS.....	51
Figure 6: PM _{2.5} concentrations product of the modeling using Geos-Chem.....	52
Figure 7: Correlation of 2015-2020 daily concentrations for each of the AQS monitoring stations when compared to GEOS-Chem.....	54
Figure 8: The bias estimation of the modeled PM _{2.5} concentrations relative to the AQS station measurements for model runs with and without the inclusion of the GFAS inventory.	55
Figure 9: Correlation of 2015-2020 third-day concentrations for each of the IMPROVE monitoring stations when compared to GEOS-Chem.....	57
Figure 10: The bias estimation of the modeled PM _{2.5} concentrations relative to the IMPROVE station 3-day measurements for model runs with and without the inclusion of the GFAS inventory.	57
Figure 11: Map of the distribution of days that exceeded the EPA Standard	60
Figure A 1: Regridding approach used to obtain TROPOMI measurements with the resolution equivalent to CrIs.....	68

Figure A 2: Example of TROPOMI (left) and CrIS (right) and retrievals for the same swath.... 69

Figure A 3: Comparison of daily averages for the Western Central and Eastern regions of CrIS and TROPOMI using 0.25 degree resolution (top row) and 0.7 degree resolution (bottom row).
..... 69

Figure B 1: Map of annual total GFAS emissions for 2015-2020 (in kg). 73

Figure B 2: Daily time-series data for modeled PM2.5 by averaging values from the AQS monitoring stations within each GEOS-Chem cell..... 74

Figure B 3: Correlation between modeled PM2.5 and AQS station-based PM2.5 using average annual measurements for each year in the six-year period. 75

Figure B 4: Time-series data for modeled PM2.5 by averaging values from the IMPROVE monitoring stations within each GEOS-Chem cell. 76

Figure B 5: Correlation between modeled PM2.5 and IMPROVE station-based PM2.5 using average annual measurements for each year in the six-year period..... 77

ACKNOWLEDGEMENTS

When I joined the program, I was told there were pretty much no students left who wanted to be like their Professors, but every day I do my best to try to be like them. First and foremost, I would like to thank Peter Kareiva for being more than a mentor. Impact doesn't happen overnight. It may not always be visible, but it's making more impact than you think. I would also like to thank, Kevin Bowman and Kazuyuki Miyazaki from the NASA Jet Propulsion Laboratory for believing in me, and for making me better every day. Thank you to Harrison Levy, one of the most important elements of my journey. I would also like to thank Deepak Rajagopal for igniting my passion for energy. Thanks to Tom Gillespie, for the extraordinary leadership of the ESE program. Thanks to those who helped me with their recommendations, especially Erroll Southers, from LAPD, Sue Perkins-Grew and Bill Gross from NEI; Armando Rios-Piter (“The Jaguar”), Maria E. Barrera, Ana L. Herrera; to Rosa E. Perez, Juan Rosellon, Elias M Saga, Fernanda Briseño, Samuel Rosas, Adam Rose, Carlos Ortiz, Federico Puente, Scott Ochoa, Alejandro Nieto, Alvaro Rios-Roca, and TJ Mccarthy. Also thanks to Yang Li, Leonardo Beltran-Rodriguez, Andrew Chan, Alex Spataru, Jiyae Hwang, Daniel Weiss, Yang Li, Sofia Ramos, Wesley Newburg, and Anthony Ridgley, for their authentic desire to help. Thanks to Ellen from the English Department for helping me organize my writing. Thanks to my friend Tim from Facilities Management for pushing me to finish, and for making all-nighters much lighter. Special thanks to Miriam Marlier, for being the definition of excellence. A tough leader with the potential of giants like Michael Greenstone, Gretchen Daily, or Jefferey Sachs. And very special thanks to Pablo Saide for being an exceptional mentor who challenged me every time, showed patience, perseverance, and brought out the most productive version of me.

VITA

Oscar A. Neyra-Nazarrett

EDUCATION

University of California, Los Angeles Los Angeles, California
Doctorate in Environmental Science and Engineering. Expected 2023

- *Honors:* National Science Foundation Research Trainee (NRT-INFEWS); Full funding.
- *Related Coursework:* Remote sensing, Environmental engineering, Geophysical modeling.

The University of Southern California, Sol Price School of Public Policy Los Angeles, California
Master of Public Policy (M.P.P.) with a Certificate in Homeland Security. Obtained May 2018

- *Honors:* Recipient of the Dean's Merit Scholarship and Sener Fellowship; Full scholarship.
- *Related Coursework:* Energy and power for a sustainable future; Economics; Econometrics; Cost Benefit Analysis; Energy regulation.

The Johns Hopkins University Washington, DC
Master of Arts in Global Security Studies Dropped Out. May 2018

- *Related Coursework:* The Art and Practice of Intelligence; Homeland Security; Global Security in the historical context.

Monterrey Technological Institute Mexico City, Mexico
Bachelor of Engineering, Sustainable Development (B.Eng). Obtained December 2014

- *Honors:* Recipient of the Dean's Academic Merit Scholarship.
- *Related Coursework:* Mass Balance; Chemistry; Thermodynamics; Energy Balance; Circuits; Physics.

RELEVANT PROFESSIONAL EXPERIENCE

LISUS Technologies Inc. Marina del Rey, California
Founder and Chief Executive Officer Present

- LISUS is a Techstars backed mineral discovery company focusing on the identification of lithium deposits using satellite data. LISUS is a spin out from MIT's Engine Blueprint program and is working on building a sustainable supply chain of Lithium to manufacture Electric Vehicle batteries.

NASA Jet Propulsion Laboratory Pasadena, California
Research Associate October 2020–December 2021

- Worked on a Multi-Satellite, Multi-Species data architecture that combines data from multiple satellites to explore the potential of observing attributes of the environment that couldn't be seen with one satellite. Used data from the Soumi-NPP, Sentinel-5P, and MOPITT satellites. Validated with In-Situ data from balloons.

NASA-JPL/ UCLA Joint Institute for Regional Earth System Science and Engineering Los Angeles, California
Graduate Research Assistant June 2019 –June 2020

- Analyzed near real time data collected by NASA's satellites to assess synergistic potential. Worked with data from the AQUA and Terra satellites. Validated with In-Situ data from airplanes.

Center for Risk and Economic Analysis of Terrorism Events (CREATE) Los Angeles, California
Graduate Research Assistant August 2017 – August 2018

- Worked on multiple national security focused projects, signed a non-disclosure agreement.

Nuclear Energy Institute
Nuclear Generation Intern

Washington, DC
May 2017 – August 2017

- Data analysis related to the U.S. Nuclear Regulatory Commission’s (NRC) inspections of U.S. nuclear power plant compliance.

Generacion Respuesta (Non-Profit Organization)

Mexico City, Mexico
July 2013 – December 2015

President and Co-Founder

- Development of multiple environmental projects in Mexico and Latin-America.
- The organization received multiple awards and grew from 50 to 5,000 members.

RELEVANT RESEARCH PRESENTATIONS

- *“Wildfires: Using Satellites to Save Lives”* presented the Interdisciplinary Ph.D. Workshop in Sustainable Development (IPWSD 2020). Columbia University. April 3, 2020.
- *“Combining satellite data from MODIS, and TROPOMI to observe wildfire smoke allows the observation of particle formation processes that were unobservable with one satellite alone.”* Presented at the American Geophysical Union, Fall Meeting 2020. December 2020.

GRANTS AND AWARDS

Academic:

- **UCLA Pritzker Impact Fellow.** June 9, 2022.
- **NASA FIREX-AQ Group Achievement Award (GAA).** June 29, 2020.
- **NSF NRT-INFEWS Fellow.** UCLA. October 1, 2018.
- **Monterrey Technological Institute’s Borrego de Oro.** Mexico City, 2014.

Entrepreneurship:

- **USC Maseeh Entrepreneurship Competition.** Runner-Up. \$15k in legal expenses.
- **Harvard Venture Incubation Program.** Spark Entrepreneurship grant. June 15, 2021.
- **MIT Cleantech Venture Competition.** Selected Semi-Finalist out of 182 Start-Ups. March 4, 2021
- **UC Easton Technology Competition.** Venture Selected Finalist. March 25, 2021.
- **ASU Innovation Open Competition.** Venture Selected Finalist. December 8, 2021.

Non-Profit:

- **Mexico State’s Environmental Leadership Group Award to Generacion Respuesta.** State of Mexico, 2014.
- **Mexico’s Youth Talent of the Year by the Magazine Reader’s Digest Mexico.** Mexico City. November 2013.

SOFTWARE SKILLS

Software: Python, Amazon Web Services, MATLAB, Linux, C#.

Statistical Software: R, STATA, Excel-Macro, SENSIT, Crystal Ball, SimVoi, TreePlan.

Energy and Climate Software: NREL System Advisor Model, The Berkeley Model, HOMER Energy.

OTHER SKILLS

General Skills: Grant Writing, Entrepreneurship, Fundraising, Advanced Sensing, Public Speaking.

Analytical Skills: Life cycle Analysis, Risk Analysis, Regression Analysis, Economic Analysis.

Languages: *Spanish* (High); *English* (High); *Portuguese* (High); *French* (Intermediate).

Others: Marathon, and Ironman 70.3 finisher.

Chapter 1 Introduction

Sophocles once said that every man sees things far off but is blind to what is near. This is reflected today in how we sometimes neglect the clear and present dangers of wildfires, despite their impacts constantly being highlighted in the news, we have yet a lot to do to understand the behavior of these events and to improve the technologies we use to study them.

Wildfires have increased significantly over the past decade (Iglesias, Balch, and Travis 2022) with the year 2020 being unusually devastating to the United States. This was particularly relevant to the western U.S. where the Wildfires damaged over 10,000 structures (National Interagency Fire Center 2020). The 2020 wildfire season reported over 4.2 million acres burned in California (Cal Fire 2023), the largest area ever recorded in the history of the state. In Oregon and Washington, the fires burnt 1.1 million and .84 million acres during the year (Northwest Interagency Coordination Center 2021). Given the relevance and magnitude of such an event, it is necessary to understand its impact and to identify ways to improve scientific measurements particularly those retrieved from space. Larger wildfires will continue to catalyze ecosystem changes, transforming the global climate and exposing entire populations to dangerous emissions. Hence, it is critical that satellite retrievals are validated and improved in order to properly model the effects of particulate matter from wildfires. This dissertation seeks to harness a multi-satellite synergy algorithm and a chemical transport model to assess the environmental impact of the pivotal wildfires of 2020 in the Western U.S.

Satellite data has been critical for analyzing wildfire emissions and has the potential to mitigate future wildfire threats. The observation power of modern satellites is almost unprecedented given

the history of satellite potential. Almost instantly, satellites can tell where wildfires are taking place, how big they are, and can be used to estimate what emissions they are producing, if they are approaching urban areas, and even what kind of fuel they are burning. Some drawbacks to utilizing satellite methodology include the possible effects of smoke contamination (Ye et al, 2022), uncertain data retrievals, and sensor-specific data limitations. Satellites, nonetheless, offer major advantages to in-situ as it is difficult to install in-situ monitors in remote locations, and to make sure they remain operational during times of duress such as major wildfire events. They also have significant advantages in their global scale of coverage and long-term observation.

Furthermore, the use of multiple satellites in conjunction offers the potential to observe with better precision attributes of wildfires, without having to launch new instruments, a concept called satellite synergy. A synergistic scheme refers to an algorithm that combines observations from two or more spectral ranges, either simultaneously or in a hierarchical manner, to achieve a more precise result than when these retrievals are used independently. Successions of satellite platforms orbiting in proximity, exhibit great potential for improved observation by concentrating sensors on a given area. (Malina et al. 2022; J. Landgraf and Hasekamp 2007; Luo et al. 2013; Cuesta et al. 2013; Fu et al. 2018; 2016; H. M. Worden et al. 2007; J. R. Worden et al. 2015; Deeter et al. 2014). Although using satellite synergies can lead to improved measurements, the approach is rarely utilized correctly. Data retrievals are usually performed independently per instrument, and the retrieved products are merged as processed imagery called posteriori. In this context, there is a strong need to formally apply the theory of synergistic processes and to go beyond the combination of images (Aires et al, 2011). Combining retrievals from multiple instruments has proven useful already, with multiple projects demonstrating that a multiple-sensor synergy can lead to greater accuracy than using just one sensor. (Fu et al, 2018;

Yan et al, 2016). This project aims to build upon a technique that has shown potential but has not been extensively executed before.

The use of satellite synergies has proven formidable in the study of a multitude of applications and the method could be invaluable to study dynamic events such as wildfires. Wildfires can rapidly change in location, duration, and intensity. However, satellites are ideally suited to monitor them because they can cover vast areas and utilize various sensors that capture data across different spectra and at different times. Hence, the use multiple satellites in conjunction serves as a foundation upon which the study of wildfires can be refined.

While the potential of satellite synergies to produce better measurements is evident, its implementation is challenging. Differences in orbits, timing, and resolution pose significant challenges to the successful construction of a multi-satellite observational system (Aires et al, 2011). Each of these attributes can only be observed independently, given that this information comes from instruments carried in satellites that are designed with particular purposes and capabilities. The combination of these factors creates challenges. Some satellites retrieve data from different orbits or times, producing unsynchronized imagery. Merging their data asynchronously has the potential to create spatial and temporal mismatches of imagery (Rogers and Yau 1989). Furthermore, differences in resolution, accuracy, vertical sensitivity, and spectral capabilities need to be considered. This is particularly challenging in the context of wildfires, as emissions generated by a wildfire might be substantially different in the morning and in the afternoon due to changes in wind speed, moisture, solar radiation, and temperature (Tang et al. 2022). Hence, just like it was done in this study, it is critical to construct comprehensive

architectures and validate them against in-situ measurements to produce better retrievals through satellite synergies.

The ability to produce measurements through satellite synergies, and therefore improve understanding of wildfire attributes will enhance the field's ability to model wildfire effects. This is because satellite data serve as input to models, hence better inputs through synergies are relevant to produce better outputs when assimilating satellite measurements with other inputs in Chemical transport models (CTMs).

CTMs provide a lens through which the spread and interaction of pollutants in the atmosphere can be simulated. Use of these models is majorly important in the field because these chemical transport models act as a bridge, assimilating different inputs and simulating its geophysical interaction with other inputs. These models are based on physics and can provide information on emissions, transport, and chemistry in areas without monitors. Nonetheless, when it comes to measuring ambient concentrations, models tend to be less precise than monitors (Reid et al. in 2019). This limitation is primarily a result of uncertainties within the datasets used as inputs. However, models do provide a distinct advantage in their ability to quantify emissions linked to wildfires (Zhang et al. 2020; Jia Coco Liu et al. 2017), a capability that monitors cannot achieve.

A major issue among existing models is uncertainty regarding the treatment of smoke, which results in inexact predictions (Ye et al 2021). To address such uncertainty, it is critical to provide better inputs for air quality models aiming at improving estimates of chemical concentrations and at better attributing the origin of these emissions. Understanding emission sources is particularly

relevant, as smoke from wildfires can be more toxic than other smoke, and as it is difficult to distinguish between emissions from fire-specific smoke and smoke from multiple sources.

Better measurements could lead to better models. When fed with the advanced data gleaned from multi-satellite analysis, CTMs become even more powerful, offering a dynamic framework for improved forecasting, monitoring, and strategic planning. And better models have the potential to revolutionize public health approaches to wildfire analysis. Their ability to differentiate what is attributable to wildfires versus the background can streamline scientific efforts to focus on wildfire-specific damages and how to best mitigate them. This is critical information which will, when made predictable and more exact, help policymakers make decisions to minimize human exposure during high concentrations. This includes providing early warnings to vulnerable populations (Makkaroon et al. 2023), protecting at-risk groups such as agricultural workers (Marlier et al. 2022), and allowing policymakers to reevaluate and potentially increase PM_{2.5} thresholds during wildfire events. All of these potentially saving thousands of lives.

More accurate understanding of the emissions through models offers the ability to provide insights to mitigate negative impacts on the environment, and particularly on public health. One major impact of wildfires is their production of fine particulate matter, PM_{2.5}, which contributes to the deterioration of global air quality. “Particulate matter” is the catch-all term for particles and droplets that are present in the air, both in solid and liquid form. and includes both PM₁₀, particles with diameters 10 mm and smaller, and PM_{2.5}, with diameters 2.5 mm and smaller (EPA 2018a). Fine PM can consist of soot, organic carbon compounds and inorganic compounds (Hanninen et al. 2009). Its small size allows PM to infiltrate deep into the lungs, even entering

the bloodstream. High levels of PM_{2.5} have been found to cause respiratory problems and can enter the bloodstream, ultimately causing premature deaths.

The impact of wildfires on PM_{2.5} levels in existing literature is well-established: a plethora of scientists have identified wildfires as a major contributor to PM_{2.5} emissions (Ammann et al. 2001; Dennis et al. 2002; Lighty et al. 2000; Sapkota et al. 2005; Coco-Liu 2016). Some suggest that wildfires are responsible for up to 18% of total PM_{2.5} air emissions in the United States (Phuleria et al. 2005). It is also known that fires directly alter the radiative budget of the atmosphere by increasing greenhouse gasses and atmospheric aerosol burdens and by modifying surface albedos via alteration of vegetation coverage (Sena et al 2013, Carter et al 2020). Aerosol emissions from fires can indirectly modify cloud properties, affecting the climate. (Ward et al 2012, Hamilton et al 2018). In addition to these impacts, of course, fires pose major air quality and health concerns from wildfire smoke (Dittrich and McCallum 2020). Based on all of this known potential for serious health and environmental damage, it is crucial that the scientific community better understand the emissions of PM_{2.5} that are attributable to Wildfires through better models.

Globally, wildfires cause an estimated 339,000 deaths annually, with regions like sub-Saharan Africa and south-east Asia being heavily affected (Johnston et al., 2012). However, the comprehensive health impacts of wildfires, including increased respiratory morbidity and mortality rates (Youssouf et al. 2014; Liu et al. 2015; Reid et al. 2016; Cascio 2018), remain under-reported and insufficiently quantified due to various challenges, being exposure misclassification one of the most relevant. Wildfires have a disproportionate effect on the most

vulnerable populations, particularly the elderly, people with pre-existing cardiopulmonary conditions, smokers and individuals with smaller airways (Yousouff, 2014).

Wildfires are an increasing threat to the environment and human welfare in the modern age and remain highly relevant in broader discussions of climate change. Current understanding of their damage potential, even as measured by satellites, is limited due to a slew of complicating factors: remote wildfire sites, unreliable satellite coverage, and major data complications due to smoke coverage. It is critical that we enhance satellite retrievals for the sake of accurate emission data. By doing so, we can achieve better modeling to understand the significance of wildfires and thus, respond more effectively. This dissertation seeks to harness a multi-satellite synergy algorithm and a chemical transport model to assess the atmospheric composition changes as well as the public health impact of wildfires. In Chapter 2, we analyze CO patterns during the 2020 wildfires using a synergy of CrIS and TROPOMI retrievals and validate it against various instruments. In Chapter 3, we employ GEOS-Chem, a CTM, to estimate the PM_{2.5} emissions attributable to wildfires in the Western U.S. and evaluate their impact on the states in said region. Beyond wildfires, the aim of this study is to serve as a groundwork to advance our understanding of wildfire dynamics and their consequences so we can protect our planet and those who live on it.

Chapter 2 A multi-satellite synergy algorithm to assess and validate CO measurements during the wildfires of 2020

2.1 Abstract

The 2020 wildfire season in the western U.S. was historic in its intensity and impact on the atmosphere. This study aims to characterize the sensitivity to carbon monoxide (CO) of two satellite instruments (CrIS and TROPOMI) during these wildfires including their spatial, temporal, and vertical patterns. Our results show that the Western U.S. displayed significantly higher daily average CO columns compared to the Central and Eastern U.S., with TROPOMI reporting higher values near the fire sources than CrIS; associated with stronger contributions of close to surface concentrations to the total column. Both satellites showed consistent values downwind related to more lofted plumes. Temporally, TROPOMI CO column peaks were delayed relative to Fire Radiative Power (FRP), particularly during the intense initial weeks of September.

Satellite retrievals were validated using TCCON and NDACC's FTIR CO column estimates, showing Normalized Mean Errors (NME) for CrIS and TROPOMI to be typically below 24% and 32% across Boulder, Colorado, Park Falls, and Pasadena. However, there were notable differences in magnitude at Pasadena likely associated to sharp spatial gradients due to topography and proximity to a large city, which is consistent with previous research. In-situ CO profiles from AirCore showing an elevated smoke plume for September 15, 2020, highlighted consistency between TROPOMI and CrIS CO columns for lofted plumes, even when the CrIS predicted profile deviates from observations.

The study demonstrates that both CrIS and TROPOMI provide complementary information on CO distribution. CrIS's sensitivity in the lower free troposphere, coupled with TROPOMI's effectiveness at capturing total columns, offers a more comprehensive view of CO distribution during the wildfires than each retrieval by itself. By combining data from both satellites as a ratio, we can potentially extract more detailed information about the vertical location of the plumes. This approach can enhance air quality models, improve vertical estimation accuracy, and establish a new method for assessing lower tropospheric CO concentrations during significant wildfire events.

Keywords: satellite synergy; carbon monoxide; TROPOMI; CrIS; TCCON; AirCore; NDACC; wildfire; retrieval.

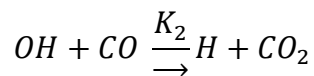
2.2 Introduction

During the period of global lockdown, satellites remained operational and proved to be an indispensable tool for characterizing the spatiotemporal distribution of gases and aerosols at a global scale (Laughner et al. 2021). However, the effectiveness of satellite observations could have been impaired by uncertainties caused by unusually high emissions from wildfires, vertical transport of wildfire plumes, and heavy smoke (Ye et al., 2022). The 2020 wildfire season in the United States presented an opportune case study to determine the degree of influence that thick smoke may have on the accuracy of remote sensing data. Unlike previous years, the 2020 season resulted in a record-breaking increase in the amount of land burned in Western U.S. which resulted in strong local, regional, and continental impacts of gases and aerosols emitted (Albores et al. 2023).

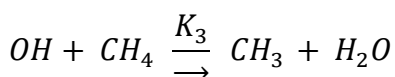
The wildfires of 2020 were a major source of carbon monoxide (CO), exceeding three times the 2001–2019 average CO emissions. (Albores et al. 2023). Wildfires can generate large amounts of CO due to incomplete fuel combustion, biomass burning, and hydrocarbon oxidation. Over 10% of global CO emissions from wildfires occur in middle and high latitudes. (Langmann et al. 2009). CO is an excellent atmospheric tracer for incomplete combustion (Martínez-Alonso et al. 2020). The presence of CO is highly relevant to climate change for two main reasons. Firstly, it reacts with the hydroxyl radical (OH), which is the primary oxidant of CO (Eqn. 1). This reaction results in the formation of greenhouse gases such as carbon dioxide and tropospheric ozone, both of which contribute to global warming. Secondly, since OH is responsible for removing CO from the atmosphere, an increased presence of CO means less OH is available to scavenge other greenhouse gases such as methane (Eqn. 2). This dynamic enhances the

atmospheric lifetime of these gases, impacting the atmosphere's ability to self-cleanse. (Seinfeld and Pandis 2012; Lelieveld et al. 2016).

(EQ1)



(EQ2)



Tropospheric CO has a mean lifetime of approximately 1 to 2 months (Seinfeld and Pandis 2016; Pfister et al. 2008; Intergovernmental Panel On Climate Change 2023), enabling it to withstand both horizontal and vertical transport while remaining unmixed. As a valuable tracer, CO is utilized to observe the transport, origins, and removal of polluted plumes.

2.2.1 Use of satellite retrievals to study CO

Satellite retrievals play an essential role in studying atmospheric composition, particularly in monitoring CO. This is because they cover a wider area, complementing the more localized observations of ground-based networks such as the Total Carbon Column Observing Network (TCCON) and the Infrared Working Group of the Network for the Detection of Atmospheric Composition Change (NDACC-IRWG). This expansive coverage is crucial for monitoring atmospheric phenomena on a global scale. While ground-based networks provide precise

measurements at specific locations, satellites offer broader data collection over large areas, which enhances our understanding of atmospheric dynamics.

Various satellites can be used to measure carbon monoxide through the estimation of the radiation they absorb. The most widely used and long-standing instrument for this purpose is the "Measurements Of Pollution In The Troposphere" (MOPITT) sensor, which is onboard the NASA Terra satellite and has been in operation since 2000 (Drummond et al. 2010). MOPITT utilizes near-infrared (NIR), thermal-infrared (TIR), and multispectral (TIR+NIR) radiances to achieve its objective (Buchholz et al. 2017)

In addition to MOPITT, other satellite instruments built to measure CO in the thermal infrared spectral regions include the Infrared Atmospheric Sounding Interferometer (IASI) (Clerbaux et al. 2009) the Tropospheric Emissions Spectrometer (TES) (K.W. Bowman et al. 2006), the Cross-track Infrared Sounder (CrIS) (Bloom 2001) and the Atmospheric Infrared Sounder (AIRS) (Fu et al. 2018) All of these instruments, with the exception of AIRS, use optimal estimation approaches to retrieve CO columns from measured radiances. Additionally, all have shown consistent hemispheric CO variability when compared to MOPITT retrievals (Buchholz et al. 2017). The disadvantage of this family of instruments is that measuring concentrations near the surface in the spectral bands they detect can be difficult (Kevin W. Bowman et al. 2002). In contrast, other types of infrared (IR) equipment, such as TROPOMI, typically provide superior insights into the lower troposphere but are unable to extract species above around 30km.

The TROPOMI instrument uniquely derives CO atmospheric columns through observations in the NIR (T. Borsdorff et al. 2018). Because of the spectral range in which it operates, TROPOMI can retrieve a CO column that captures most of the CO across the upper and lower troposphere demonstrating superior sensitivity near the surface compared to sounders such as CrIS. Using TROPOMI and CrIS, both recently deployed instruments, we benefit from their complementary capabilities and their strategic co-location on the same satellite train. This offers enhanced synergistic potential and the opportunity for the development of future joint retrievals, making them uniquely suitable to our study.

2.2.2 Previous work validating CrIS and TROPOMI CO retrievals

There is limited literature on the joint validation and assessment of the synergistic potential of TROPOMI and CrIS. Prior studies have validated CO retrievals from CrIS or TROPOMI by comparing them independently with other satellite datasets. (H. M. Worden et al. 2013; Martínez-Alonso et al. 2014; George et al. 2015; Martínez-Alonso et al. 2022), aircraft based vertical profiles (Martínez-Alonso et al. 2020; 2022), and ground measurements (Dammers et al. 2017; Hedelius et al. 2018). These studies generally found that both CrIS and TROPOMI exhibit a positive correlation with other satellites, airborne data, and ground measurements. However, at the surface level, CrIS typically displays lower sensitivity, resulting in overestimation in low-concentration conditions and underestimation in higher atmospheric concentration conditions (Dammers et al. in 2017).

In contrast with CrIS, there is more extensive literature evaluating TROPOMI CO retrievals through studies comparing them with satellite, ground-based and airborne instruments and reanalysis of atmospheric composition. In multi-satellite instrument comparisons, one study (Martínez-Alonso et al. 2020) analyzed TROPOMI CO data from November 2017 to March 2019, comparing it with MOPITT satellite data and Atmospheric Tomography mission (ATom) aircraft data. This study found that TROPOMI CO retrievals over land show an average relative bias and standard deviation of $-3.73\% \pm 11.51\%$, $-2.24\% \pm 12.38\%$, and $-3.22\% \pm 11.13\%$ compared to MOPITT's TIR, NIR, and multispectral products, respectively. The study also revealed good agreement in temporal and spatial patterns between TROPOMI and MOPITT data. Another study (Martínez-Alonso et al. 2022) presented an intercomparison of TROPOMI CO measurements with MOPITT, including validation using vertical profiles from balloon-borne AirCore measurements. This study reported mean MOPITT/AirCore total column bias values and their standard deviation as 0.4 ± 5.5 , 1.7 ± 5.6 , and 0.7 ± 6.0 molec/cm² for MOPITT's thermal-infrared, near-infrared, and multispectral retrievals, respectively. It also highlighted that TROPOMI can retrieve CO under both clear and cloudy conditions with a relative bias and standard deviation of $2.02\% \pm 11.13\%$ in cloudy conditions, after accounting for TROPOMI's vertical sensitivity to CO.

Regarding ground-based instrument comparisons, a study (Shah et al. 2021) validated TROPOMI's operational CO products over about three years using ground-based data from the Total Carbon Column Observing Network (TCCON) and the Infrared Working Group of the Network for the Detection of Atmospheric Composition Change (NDACC-IRWG). They addressed uncertainties in a priori alignment and smoothing in the validation process. Other approaches (Yang et al. 2020) have, compared FTIR measurements at Xianghe with co-located

TROPOMI satellite and ground-based Orbiting Carbon Observatory-2 (OCO-2) observations, an instrument that adheres to TCCON guidelines. Both studies found proper representation of TROPOMI. Moreover, TROPOMI retrievals have also been found consistent with atmospheric composition reanalysis (T. Borsdorff et al. 2018), further affirming the reliability of TROPOMI CO retrievals in various comparative studies.

2.2.3 Satellite synergies.

The concept of "satellite synergy" entails the fusion of data from multiple satellite sensors, and satellite synergies to observe attributes of the environment that are not discernible with a single satellite instrument. Joint retrieval, on the other hand, involves considering the interrelations between distinct geophysical parameters. Studies have demonstrated that the integration of data from multiple sensors is highly advantageous, particularly within the context of joint retrievals (Malina et al. 2022; Mettig et al. 2022; J. Landgraf and Hasekamp 2007; Luo et al. 2013; Cuesta et al. 2013; Fu et al. 2018; 2016; H. M. Worden et al. 2007; J. R. Worden et al. 2015; Deeter et al. 2014). One recent study demonstrated the effectiveness of joint retrievals using CrIS-TROPOMI with a focus on ozone (Malina et al. 2022). However, no study has been conducted to assess the synergistic potential of combining UV and IR spectral measurements for CO using CrIS and TROPOMI.

There is a gap in existent literature because there are no previous studies that have validated the synergistic potential of TROPOMI and CrIS when observing Carbon Monoxide in the presence of high intensity wildfire events. The present study aims to address this gap through the validation of such synergy using ground-based remote sensing and in-situ vertical profiles. Our study has two key objectives, first, it aims to understand the underlying differences in the way CrIS and TROPOMI observed CO during the megafires. Second, it aims to understand how satellite measurements compare to ground-based reference measurements during such an event, and the scientific implications of such comparisons. This work is organized as follows. In section two we describe the data and method used to homogenize the data from all the instruments. In the third section we present and discuss the results of our study through temporal, spatial, and vertical lenses, and in section four we present the conclusions and future directions of this study.

2.3 Data and Method

2.3.1 Satellite CO retrievals

In this section, we provide a summary of the features of the two satellite CO products we utilized to perform our study and provide an overview of its characteristics.

Table 1: Overview of the Satellite CO products assessed.

Dataset	TROPOMI	CrIS
Equatorial crossing time	13:30 LST	13:30 LST
Nadir resolution (km)	Up to 7x5.5 km ²	14x14 km ²
File Name	L2__CO__	CRIS_L2-CO
Swath Width (km)	2600 km	2200 km
Satellite	Sentinel 5P	Suomi-NPP

Prior	TM5 model	MUSES-TES
Estimation	Tikhonov regularization	Optimal Estimation
Reference	(ESA 2023)	(Fu et al. 2016)

2.3.1.1 CrIS CO

We use CO retrievals from the Cross-track Infrared Sounder (CrIS) aboard the Suomi National Polar-Orbiting Partnership (S-NPP) satellite (also referred to as NOAA-19), which has been providing data since 2015. The data of this instrument was obtained using the TES algorithm from JPL (K.W. Bowman et al. 2006), with data produced operationally at 0.7 degree resolution to save computational costs. We tested the impact of resolution on our data by comparing its consistency with reprocessed data of higher resolution (0.25 degree) for the period of Sept 11-15, 2020, which displayed the highest CO concentrations in the fire season. We analyzed daily averages for the same geographical region at both resolutions and found that using 0.7 degree resolution provided similar results, as demonstrated in Figure A3. Nevertheless, utilizing this product could introduce some uncertainties since its coarser resolution might result in the omission of certain relevant values in space.

2.3.1.2 TROPOMI CO

The other satellite instrument utilized was TROPOMI. It is a push-broom imaging spectrometer carried by the Sentinel 5P Satellite from the European Space Agency (T. Borsdorff et al. 2018). TROPOMI has a wide swath width of 2600 km which provides quasi-global daily coverage. It measures radiances in the ultraviolet, visible, and solar-reflected infrared ranges (Martínez-Alonso et al. 2022). Its total CO column values are obtained from measurements of reflected solar infrared radiation in the 2.3 μm spectral band. One advantage of TROPOMI is its ability

retrieve CO over land in both clear and cloudy conditions (Jochen Landgraf et al. 2016). The reason TROPOMI is capable of this is due to its ability to retrieve parameters such as cloud height and optical thickness concurrently with trace gas columns. These parameters are then used to estimate partial CO columns above cloud tops using scaled reference profiles from the global chemical transport model TM5 (Krol et al. 2005).

The recent operational changes to the Copernicus Sentinel-5P have enhanced the resolution of TROPOMI, providing data at approximately 7×5.5 km² since August 2019, which has been beneficial for our study that utilizes 2020 data (Jochen Landgraf et al., 2016).

2.3.2 Reference Data

2.3.2.1 Satellite Fire Radiative Power retrievals from VIIRS

To track fire activity, we used Fire Radiative Power (FRP) data from the Visible Infrared Imaging Radiometer Suite (VIIRS) instrument carried by the Suomi NPP Satellite. Such instrument offers the advantage of providing daily globally active fire data (Csiszar et al. 2016). Specifically, we used S-NPP VIIRS with an imagery-resolution of 375 m-pixel (Wolfe et al. 2013). S-NPP VIIRS operates on a sun-synchronous orbit, making a pass over the equator at around 1:30 local time during its descending orbit and at approximately 13:30 local time during its ascending orbit. The Fire Radiative Power (FRP) metric quantifies the total amount of radiant energy released by the fire and is expressed in megawatts (MW) at the pixel level. The product (VNP14IMGTDL_NRT) is available at the Fire Information for Resource Management System (FIRMS) database.

To evaluate fire activity, we analyzed cumulative Fire Radiative Power (FRP) using daily daytime measurements grouped into 400-second segments. This method accurately measures wildfire intensity, rather than wildfire activity, by summing FRP values within each 400-second interval. Higher sums within these segments suggest more intense fire activity. The utilization of short intervals facilitates capturing rapid fluctuations in fire intensity, which could be missed through a more aggregated analysis. Given that the majority of fire activity occurred in the Western U.S. we limited the FRP data extraction to this region.

2.3.2.2 Ground-based TCCON CO measurements

The TCCON Network is integrated by a group of ground-based Fourier transform spectrometers (FTSs) and is currently the state-of-the-art reference measurement to validate total column measurements through remote sensing (J. L. Laughner, 2023). The FTSs in the TCCON network use direct solar absorption spectra in the NIR spectral range to obtain precise column-averaged measurements of atmospheric constituents, such as CO₂, CH₄, and especially CO, in addition to other species (Wunch et al. 2011; Sha et al. 2021). TCCON has been effectively used to validate trace gas data products from satellite instruments such as GOSAT, OCO-2, MOPITT, and SCIAMACHY (Sha et al. 2021).

We use data from three stations located in the states of Oklahoma, California, and Wisconsin (Lamont, Pasadena, and Park Falls respectively); Table 2 outlines the geographical specifications of such locations. To evaluate CO column measurements from satellites, we use the official TCCON XCO product, in wet mole fractions and convert them to columns as outlined in Section 2.4.3. The TCCON data were obtained directly from <https://tccodata.org/> (last access: 18 Jan 2023).

Table 2: Ground based Fourier transform spectrometers (FTSs) and corresponding network. Four FTIR sites were used in this study, three corresponding to TCCON and one to NDACC.

Attribute	Boulder	Pasadena	Lamont	Park Falls
Latitude	40.04° N	34.14° N	36.60° N	45.95° N
Longitude	105.24° W	118.13° W	97.49° W	90.27° W
State	Colorado	California	Oklahoma	Wisconsin
Network	NDACC	TCCON	TCCON	TCCON
Reference	(Ortega et al. 2019)	(Wennberg et al. 2023)	(Wennberg et al. 2023)	(Wennberg et al. 2023)

2.3.2.3 Ground-based NDACC-IRWG CO retrievals

We used data from the Boulder station of the Network for the Detection of Atmospheric Composition Change (NDACC), as provided by Ortega and colleagues. NDACC encompasses more than 20 stations, each outfitted with high-resolution Fourier transform spectrometers. These devices are adept at capturing solar absorption spectra within the mid-infrared (MIR, 2–14 μ m) spectral range, a methodology outlined in prior studies (Buchholz et al. 2017).

NDACC retrieves CO measurements in the MIR spectra using three narrow spectral windows in the CO fundamental absorption band as outlined in previous studies (C. P. Rinsland et al. 2007; Buchholz et al. 2017; Dammers et al. 2017). Because of its rigorous calibration and quality control procedures, long-term and consistent data record, high-quality data, global network of stations, traceability to SI standards, and open access to data, NDACC has been extensively used to validate satellite data in prior studies (Buchholz et al. 2017; Olsen et al. 2017; Dammers et al. 2017; Hochstaffl et al. 2018; Hedelius et al. 2018; Tobias Borsdorff et al. 2020).

2.3.2.4 Balloon based CO retrievals using Aircore

We acquired data on the chemical composition of vertical profiles through the use of the AirCore instrument (Karion et al. 2010). Profiles were retrieved by Baier and colleagues, utilizing data from two specific dates, August 12th, 2020, and September 15th, 2020; with launches conducted in Boulder, Colorado.

The AirCore, a balloon-borne atmospheric sampling tool developed by NOAA, features a unique design comprising an elongated, coiled tube. Its primary function is the passive acquisition of atmospheric samples during high-altitude balloon flights. To produce a vertical sample, AirCore is charged with a preset gaseous blend, or "fill gas," that comprises average atmospheric concentrations of carbon dioxide (CO₂) and methane (CH₄), enhanced with slightly higher mole fractions of carbon monoxide (CO). The apparatus is designed with one end hermetically sealed and the other open to the external atmosphere, allowing the fill gas to be expelled when the balloon ascends to about 30 km above mean sea level. Following detachment from the balloon, the AirCore begins continuous ambient air sampling during its descend from the apex altitude to the terrestrial surface. When the air sample lands, a mechanism is activated to automatically shut the open end of the coil, preserving the integrity of the sample (Martínez-Alonso et al. 2022).

The AirCore data were obtained directly from

http://gml.noaa.gov/ccgg/arc/tmp/arcrepo_34Twm7/NOAA_AirCore_data_v20210813.zip (last access: Jan 5, 2022).

2.3.3 Satellite synergy

To jointly assess and validate CrIS and TROPOMI CO measurements, we used a multi-satellite synergy that included matching retrievals in space and time and comparing CO column densities obtained from both as described in the following subsections.

2.3.3.1 Temporal co-location of satellites

We used temporal co-location to match TROPOMI and CrIS data, following the methods used in previous studies (Langerock et al. 2015). For measurements to be accurate and to mitigate noise due to atmospheric changes, meaningful collocation is necessary, ensuring that sensors perceive the same location at approximately the same time. (Rogers and Yau 1989). Fortunately, S-5P (hosting TROPOMI) and S-NPP (hosting CrIS) are both in the A-Train Constellation, which implies that one satellite overpasses the earth right before the other, with an equatorial crossing time of roughly 1:30 p.m. local time and an overpass time difference of less than 5 minutes (Latsch et al. 2022). Because both sensors are in the same train and have similar swaths, measurements that meet the temporal condition will likely have a match for the spatial criterion.

Despite being in the same train, co-locating TROPOMI and CrIS data creates difficulties due to their heterogeneous nature and the spatial and temporal constraints that must be met. To address this, we developed a collocation approach that simplifies data processing. First, we extract TROPOMI files by swath crossing the continental United States. The data is then filtered and organized based on the hours the satellites pass over the continental US, and temporal matching with CrIS daytime value retrievals is performed. Hence, we obtain measurements both temporally and spatially homogeneous, albeit at varying resolutions.

To ensure the reliability of the data, we established additional filters. We only use daytime data for CrIS (TROPOMI data are daytime only) and quality filter with a minimum threshold of 0.5 were used for each of the two retrievals, 'qa_value' for TROPOMI and 'Quality' for CrIS.

2.3.3.2 Re-gridding of satellite data

After performing temporal and spatial co-location of the data, the resolution of the data is homogenized for each day when there is a match between CrIS and TROPOMI data. Since CrIS pixels (0.7 or 0.25 degree) have a larger size and different resolution than TROPOMI pixels (7 km × 3.5 km), TROPOMI was regrided to the CrIS grid by using the center of each CrIS pixel, drawing a square of (0.1°) around it, and averaging the TROPOMI pixels which center falls within the square. The dataset is then stripped of all CrIS pixels that do not have associated TROPOMI pixels to only keep paired pixels.

2.3.4 FTIR Co-location

To verify the accuracy and consistency of our data, we conducted a spatial co-location process where we compared the satellite measurements with the ground-based FTIR measurements following the methodology of Sha (Sha et al. 2021). For each day, we chose the CrIS and TROPOMI homogenized observations that corresponded to the position of the ground-based reference data. By centering on the FTIR locations, we selected matching daily satellite data within a square centered at the site with a side of 1.5° (0.75° Apothem).

Once we successfully achieved spatial co-location between satellite data and FTIR, we calculated the spatial averages by obtaining an average daily measurement for CrIS and TROPOMI. However, we had multiple daily measurements for FTIR at this stage. Therefore, we filtered the FTIR data to align them temporally with the timing of the satellite retrieval overpassing times, averaging all FTIR retrievals for the corresponding hour.

The CrIS and TROPOMI column results are then compared directly to Boulder NDACC data product as it already provides column estimates (Ortega et al. 2019). Yet, to align TCCON with the other measurements, units are converted from column-averaged dry-air mole fractions to dry column through a methodology closely aligned to previous studies (Langerock et al. 2015; Kiel et al. 2016; Yang et al. 2020; Sha et al. 2021). We calculate the total dry CO column using a method similar to existent methodologies (Deutscher et al. 2010) as described in Equation 3. Specifically, we convert the surface pressure (Ps) from atmospheres of wet air into molecules per cm², recorded at the lowest vertical level of the Prior total air column. Subsequently, we estimate the proportion of this column that represents dry air to estimate the dry CO column.

(EQ3)

$$Column_CO_{Dry} = Column_Air_{wet} * XCO * Percent_Dry$$

Where

$$Column_CO_{Dry} = \frac{Prior_PS_{Surface}}{MW_{Air}} * XCO * \left(1 - \frac{X_{H2O}}{X_{CO}}\right)$$

2.3.5 Processing of Aircore data

We estimated total CO column from AirCore data applying the averaging kernels (AK) of co-located CrIS and TROPOMI retrievals to the AirCore CO profiles. For TROPOMI, we use AK in units of meters derived from a first-order Tikhonov–Phillips regularization on a logarithmic scale (Hase et al. 2004; Schneider, Hase, and Blumenstock 2006) resulting in a CO column comparable to TROPOMI CO columns. For CrIS, we use Averaging Kernels derived from Optimal Estimation as $\ln(\text{VMR})$ resulting in a smoothed profiles that take into account the vertical sensitivity of this instrument. The smoothed CO profile is then used to calculate a CO column to compare against the CrIS CO columns, but it can also be compared to the profile derived by the CrIS algorithm.

The colocation criteria requires that measurements from the two devices be collected within a time range of 12 hours or less and within a geographical proximity of 0.15 degrees or less. For both CrIS and TROPOMI, we took the average of pixel that satisfied these colocation conditions. To avoid bias we used high-resolution data processed at a granularity of 0.25 degrees for CrIS and standard high-resolution data for TROPOMI.

We conducted a vertical regridding (Langerock et al. 2015) of the AirCore data to match the levels of CrIS and TROPOMI, using pressure as a reference. Given the initial difference in vertical levels—with AirCore at 521 levels, TROPOMI at 50, and CrIS at 67—this regridding process ensured alignment with TROPOMI and CrIS. It also allowed for the application of Averaging Kernels, harmonizing the AirCore profile with the respective satellite measurement profiles.

2.4 Results and Discussion

2.4.1 Synergy Evaluation

2.4.1.1 Regional

We compared CO columns from CrIS and TROPOMI after applying the homogenization method described earlier (Section 2.3). Figure 1 shows the spatial maps of CO observed by the satellites during September 12 of 2020 for the continental U.S., which displayed one of the highest daily average CO measurements of the entire fire season. We focused on three regions: the western, central, and eastern U.S. The figure shows that concentrations in the Western U.S. were much higher than in the other two regions. Near the fire, the instruments detected different CO concentrations. Yet, TROPOMI and CrIS measurements were generally similar at locations downwind from the fires. This is further evidenced when assessing the scatterplot between CrIS to TROPOMI in the three regions (Fig. 1 right panel), with strong fit and slope close to 1 for the Central and East regions, and much wider dispersion for the Western US, going from values close to the 1:1 line up to very strong underpredictions of CrIS relative to TROPOMI.

These results could imply that close to the fires a significant fraction CO (50% on average for this day) was present in the lower troposphere as previous studies have shown that TROPOMI is better at capturing the entire column, versus CrIS, which is more sensitive in the middle troposphere (K.W. Bowman et al. 2006; Malina et al. 2022). When looking at Central and eastern US, the slopes close to one could imply that the plumes were mostly lofted in the free-troposphere and thus both instruments sensed most of the CO column. This hypothesis will be reassessed when comparing the satellite retrievals to the reference measurements in the following sections.

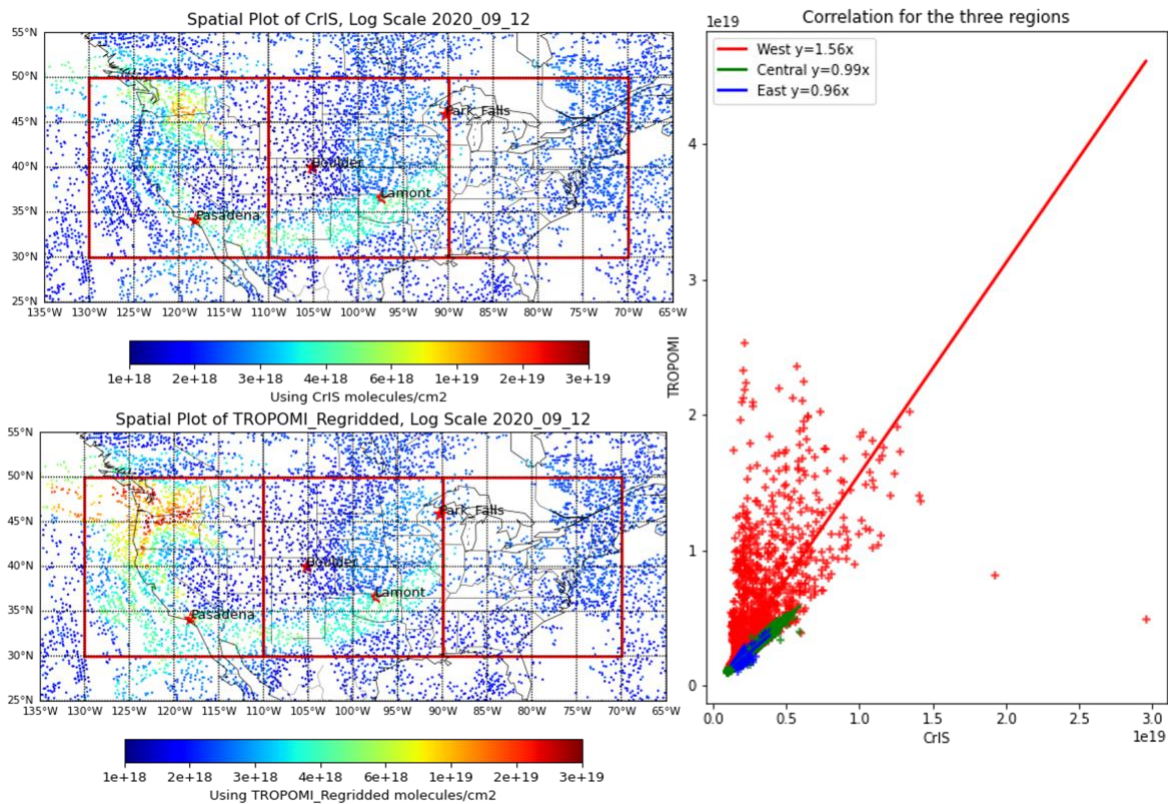


Figure 1: Left panels: Maps of CrIS high resolution data (0.25 degrees) and homogenized version of TROPOMI. The three regions of interest are shown as red squares, and ground-based sites marked with stars. Right panel: A comparison of measurements for the Western, Central, and Eastern regions of the United States.

Figure 2 displays the daily average concentrations for CrIS and TROPOMI in the three regions of interest and displays the standard deviation of such measurements for each given day. Such analysis is further complemented with FRP measurements which was included exclusively for the Western region, given that the majority of fire activity occurred in this region, and the majority of CO was transported from this region to the East.

Our temporal analysis shows that the Western region experienced much higher average CO concentrations than the Central and Eastern regions of the U.S. Figure 2 further evidences that

TROPOMI saw on average higher concentrations than CrIs during and after days with higher FRP in the Western U.S. This is of particular relevance for the first three weeks of September when TROPOMI shows not only a much higher daily average than CrIS, but also a much higher Standard Deviation. This again implies that for the most intense period, a large fraction of the smoke might be close to the surface where CrIS has low sensitivity.

CrIS and TROPOMI measurements are slightly delayed relative to Fire Radiative Power as evidenced in the CO peak for the Western U.S. In fact, the peak CO columns appear a couple of days after the days with higher FRP and when FRP had the largest decline from its peak. This shift in the peak is likely due to multiple reasons, including FRP retrievals occurring before the fires reach their maximum activity and smoke accumulating in the domain during this period. Also, as shown in Figure 1, some of the smoke was transported over the ocean and recirculated, which increases the residence time in the region and contributes to the shift.

When further evaluating the delay of CrIS relative to TROPOMI during the first two weeks of September, it can be observed that the peaks on CrIS retrievals occurs 1-2 days later than TROPOMI. The main reason CrIS does not immediately detect as high levels of CO as TROPOMI might be because CO first gets formed in the boundary layer where TROPOMI has better retrieval capabilities, and then it gets transported into higher altitudes. Hence, when there is a higher delay in CrIS matching TROPOMI CO retrievals, it could mean that a larger amount of CO is remaining in the lower troposphere. Conversely, on other days TROPOMI and CrIS peak at the same time and the column amounts are closer, which could mean that a substantial

amount of CO has moved to higher altitudes and the ratio of elevated versus surface smoke does not change drastically throughout the days.

In contrast to the western US, CrIS and TROPOMI daily averages track closely for the central and eastern US (Figure 2, bottom panels). It is likely that a large fraction of the smoke was transported through the free-troposphere, and thus both instruments captured it similarly.

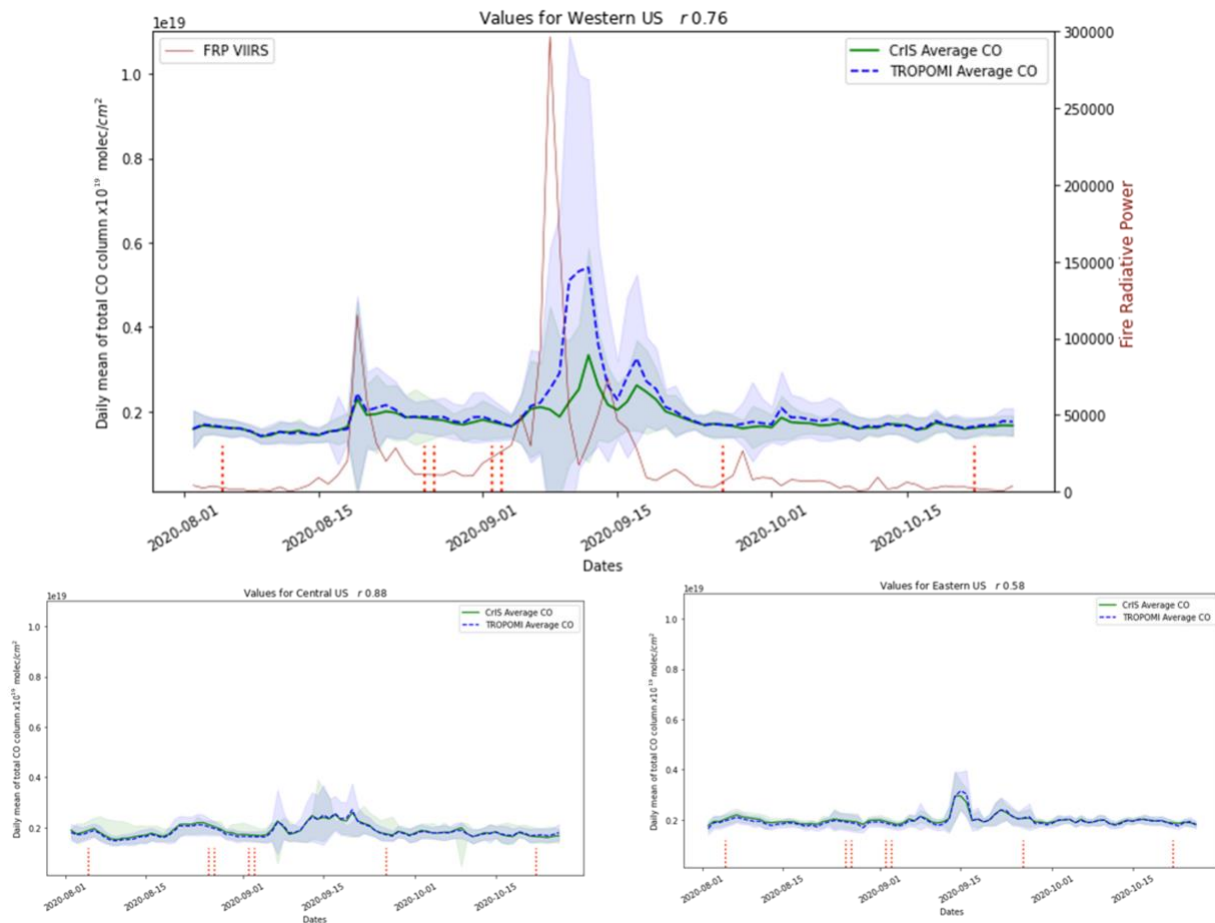


Figure 2: Daily mean measurements obtained from CrIS and TROPOMI regridded to match CrIS measurements for the Western, Central, and Eastern regions. Red dotted lines indicate days with missing data in one of the satellites. Total fire radiative power for the Western U.S. is shown as red solid line for this region.

2.4.2 Data Validation

In this section, we compare our satellite data analysis with ground-based reference measurements to illustrate and validate our findings. The temporal and spatial variations are compared against TCCON and NDACC stations. The vertical sensitivity of the satellite products is assessed using the Aircore observations.

2.4.2.1 FTIR/Satellite

Satellite measurements of CO show close agreement with the observations from TCCON and the NDACC at Boulder, Park Falls, and Lamont (Figure 3), with Normalized Bias (NMB) and Normalized Mean Errors (NME) typically below 24% and 32%, respectively for all the four sites (Table 3). However, for Pasadena, while the satellites show rapid temporal variations consistent with the TCCON observation (r 0.74 and 0.88), they show lower mean concentrations which are also reflected in the slope (\sim 1.19 and 1.32). This inconsistency aligns with existing literature on the subject (Shah et al., 2021). The likely cause of the discrepancy is the site's location in a major urban basin in Los Angeles, which is continuously affected by the urban plume. In contrast, the plume is diluted in the satellite data as it includes regions outside the basin.

As shown in Figure 3, there were a limited number of TCCON data retrievals between September 9 and September 22 of 2020 for the Pasadena site. However, one example is available for September 7th in Pasadena where TROPOMI retrievals are within the variability of TCCON which shows large values ($0.5\text{-}0.6 \times 10^{19}$ molec/cm²), while CrIS is substantially lower

($\sim 0.35 \times 10^{19}$ molec/cm²), thus corroborating that TROPOMI captures most of the column which seems to have a large fraction close to the ground as CrIS shows much lower values.

The limited number of TCCON data retrievals between September 9 and September 22 was primarily due to the observatory shutting down because of ash from a nearby fire (Bobcat). This situation was exacerbated by COVID-19 emergency's measurement constraints. Despite the difficult circumstances, satellites were able to continue functioning and gathering crucial data. However, it's essential to note that they may face unique challenges in highly polluted environments which can affect the accuracy and reliability of their data due to factors like atmospheric scattering or signal absorption. Despite these potential issues, satellites were still able to successfully collect data that ground-based observatories couldn't due to unfavorable conditions on the ground.

In Boulder, it was observed that both TROPOMI and CrIS detected an outlier on August 19 (Figure 3), with values of 0.65×10^{19} and 1×10^{19} molec/cm², respectively. However, the NDACC data for the same day showed much lower CO values (0.2×10^{19} molec/cm²). While the large satellite CO columns might have been influenced by the regional smoke and nearby fires, NDACC could have missed it given that it was a cloudy day. This highlights how cloud cover can obscure ground-based measurements and hinder the detection of smoke, which could also be the case for other stations when the plume is already uplifted. To avoid biasing our estimations, the correlation calculations do not include this outlier.

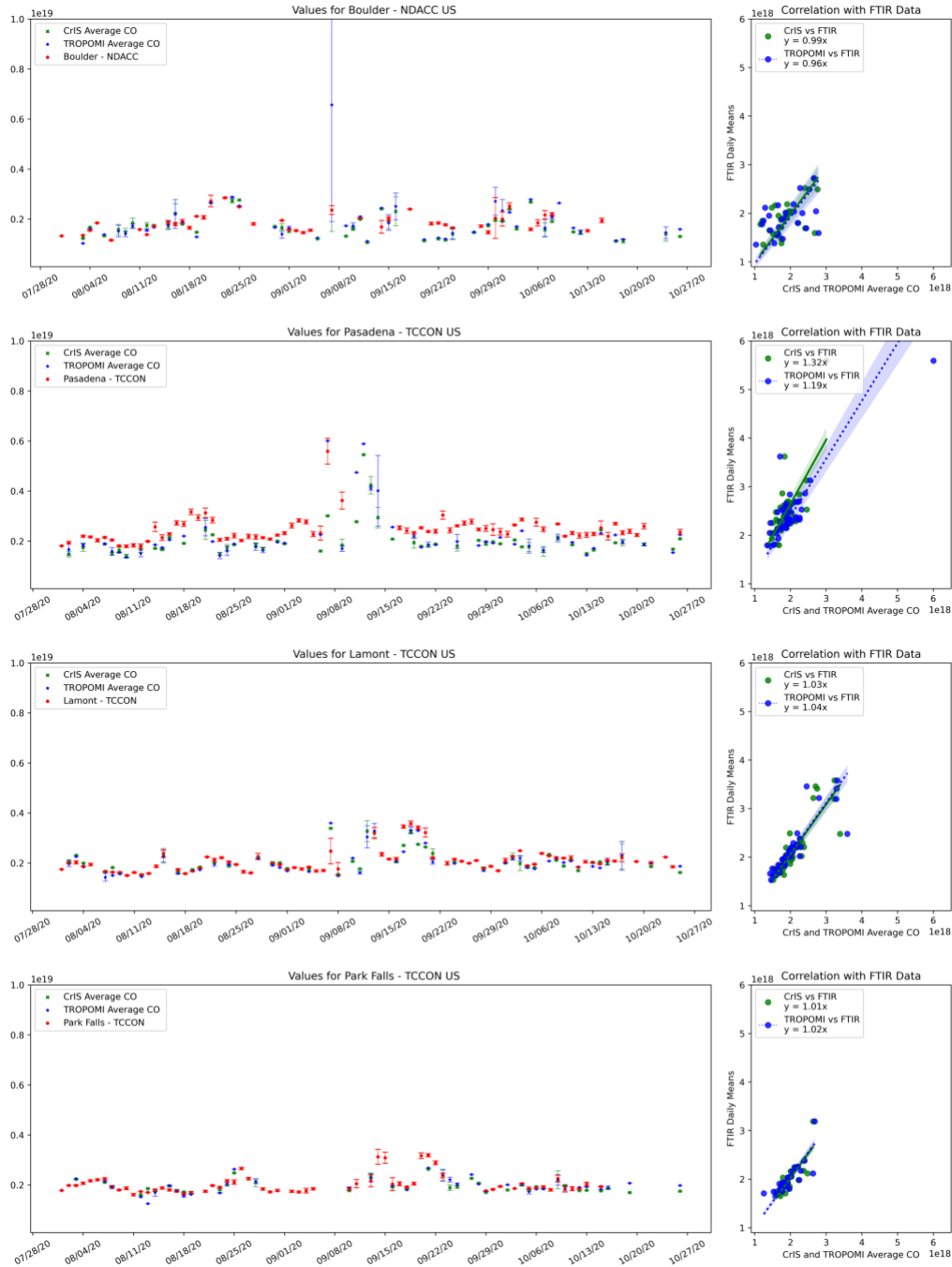


Figure 3: Daily averaged homogenized satellite CO column measurements of CrIS and TROPOMI for four FTIR locations in 2020 (Boulder, Pasadena, Lamont, and Park Falls). The right side of each figure displays correlation of pixels across the fire season with regressions, intercept adjusted to zero, and excluding an outlier in Boulder (August 19th, 2020). See text for details.

Table 3: Key statistics of average co-located satellite retrievals that correspond to each of the ground-based measurements shown in Figure 3. “N” refers to the number of samples, “r” signifies the correlation coefficient, “RMSE” stands for Root Mean Square Error, “Bias” represents the bias, “NME(%)” indicates the Normalized Mean Error in percentage, and “NMB(%)” denotes the Normalized Mean Bias in percentage. The data is organized based on the respective measurement sites and satellite products.

Product	N	r	RMSE	Bias	NME(%)	NMB(%)
Boulder Site – NDACC						
CrIS	26	0.37	1.69e+18	2.88e+17	31.91	15.03
TROPOMI	26	0.44	9.35e+17	1.53e+17	25.30	7.99
Pasadena Site – TCCON						
CrIS	44	0.74	7.23e+17	-5.90e+17	23.98	-23.98
TROPOMI	44	0.88	5.74e+17	-4.75e+17	20.07	-19.31
Lamont Site – TCCON						
CrIS	44	0.85	2.65e+17	-6.54e+16	7.68	-3.03
TROPOMI	44	0.87	2.71e+17	-9.77e+16	7.79	-4.52
Park Falls Site – TCCON						
CrIS	29	0.82	1.69e+17	-2.49e+16	6.20	-1.26
TROPOMI	29	0.81	1.90e+17	-4.94e+16	6.59	-2.49

2.4.2.2 Aircore/Satellite (Vertical)

There were two dates for which Aircore retrieved vertical profiles for the period of this study, these were August 12, 2020 and September 15, 2020. Since the fires ignited with higher intensity during September, the profile retrieved in September 15, 2020 contained an elevated smoke plume (Figure 4), while for 08/12 there was no clear evidence of a smoke plume (figure not shown). This is consistent with the Boulder NDACC site (similar location) as 9/15 shows enhanced columns $\sim 2e+18$ molec/cm² that both satellites capture well (Figure 3). CrIS, TROPOMI, and the corresponding Aircore CO column estimates all show similar values for this day (Table 4), with Aircore estimates being slightly lower. This could be due to AirCore starting

measuring at altitude, and also due to time differences as Aircore profiles are launched in the morning versus the afternoon overpass of S-NPP and S5-P.

Figure 4 shows that CrIS Aks for this day and location have high sensitivity in the lower free-troposphere, which decreases rapidly close to the surface. This is consistent with other studies that have observed peak-averaging kernels at lower altitudes, in our case at around 700 hPa. (K.W. Bowman et al. 2006; Malina et al. 2022; Mettig et al. 2022; Fu et al. 2016). The Aircore profile exhibits a CO enhancement at approximately 300-400 hPa (7-9 km). Most of the averaging kernels have some degree of sensitivity in this region, but it is above the altitude of peak sensitivity. This results in the Aircore plume being smoothed out vertically after applying the CrIS averaging kernels, losing the layered structure and showing enhancements compared to the CrIS prior throughout the free troposphere. The CO concentrations obtained from CrIS are higher than those from the prior (Figure 4). However, they tend to favor the placement of plumes at lower altitudes due to the larger magnitude of the averaging kernels at those altitudes. It's important to mention that while the CrIS column retrievals show clear enhancements (that are similar to TROPOMI) corresponding to the arrival of smoke plumes, they struggle to capture the right vertical profile due to insufficient DOFs. In conclusion, the vertical profile retrieval can struggle when placing vertical layers if that information is not contained in the prior, but nevertheless, the column enhancement is properly captured. Considering TROPOMI's enhanced sensitivity across the vertical distribution of carbon monoxide (CO), particularly near the surface, and CrIS's high sensitivity in the lower and middle free troposphere but reduced effectiveness near the surface, using a ratio of CrIS to TROPOMI column measurements emerges as a

promising method for determining the vertical placement of CO and other gases and aerosols associated to smoke. This approach capitalizes on the strengths of both instruments.

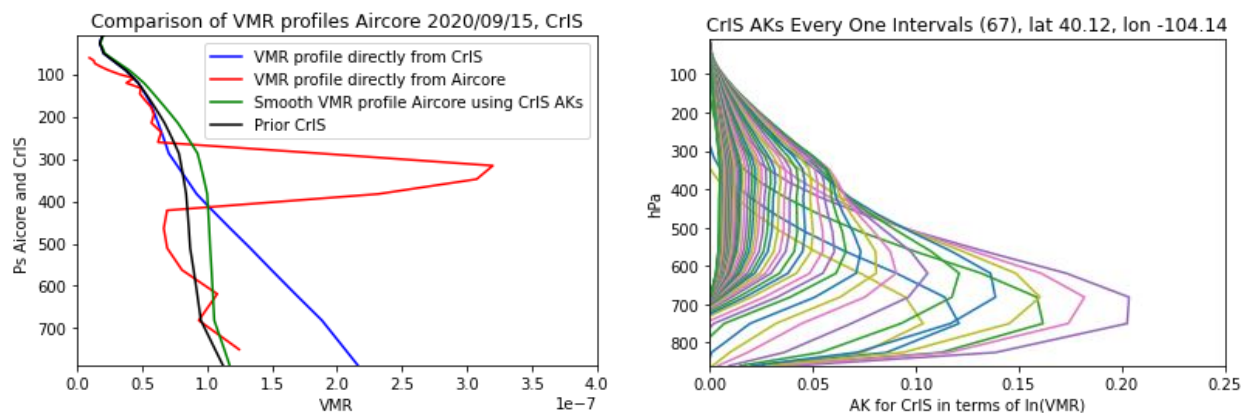


Figure 4: Left panel: vertical profiles derived from balloon-borne Aircore measurements and the corresponding co-located vertical profile from CrIS. The CrIS co-located profile’s volume mixing ratio (VMR) is depicted in blue, while the VMR of Aircore is represented in red. The CrIS prior values are shown in black, and the green line displays the Aircore vertical profile after applying the CrIS’s Averaging Kernels. Right panel: This plot depicts each row of a 67x67 Averaging Kernel matrix, selected from CrIS, based on specific geographic criteria (latitude: 40.14; longitude: -104.14). Each line represents the AK values for one of the 67 pressure levels, plotted against the corresponding pressure values.

Table 4: This table compares the column data from TROPOMI and CrIS for the location of AirCore launch. It then applies the averaged Kernels of CrIS and TROPOMI to AirCore to get the smoothed column

Type	TROPOMI	CrIS
Satellite	2.08e+18	2.09e+18
AirCore (Smooth)	1.83e+18	1.76e+18

2.5 Conclusions and future directions

To understand the differences in how CrIS and TROPOMI detected carbon monoxide levels during the 2020 wildfires, we have created a spatiotemporal satellite synergy assessment framework. This framework also evaluates how satellite measurements compare against ground-based references during such events. We examine spatial, temporal, and vertical scenarios to highlight their differences. The key findings of our framework are outlined as follows.

Spatial disparities between CrIS and TROPOMI satellite retrievals were highlighted when comparing CO columns near the Megafire's source in the Western U.S with those from the central and eastern regions. While there was a good correlation between TROPOMI and CrIS measurements at a distance, there were noticeable inconsistencies when the satellites were closer to the fire. This would support earlier studies that found that while CrIS showed higher sensitivity to the middle troposphere, TROPOMI was better able to observe the entire column (Johnson et al. 2023; Malina et al. 2022).

A significant difference in average CO concentrations between the Western U.S. and the Central and Eastern regions was found during periods of high Fire Radiative Power (FRP). Particularly in the first three weeks of September, TROPOMI consistently reported higher concentrations than CrIS in the Western U.S., suggesting substantial smoke presence near the surface where CrIS has lower sensitivity. Meanwhile, the Central and Eastern U.S. presented closely tracked daily averages between CrIS and TROPOMI, indicating a similar capture of smoke transport through the free-troposphere by both instruments. Interestingly, both CrIS and TROPOMI measurements exhibited a delay relative to FRP, with the CO peak appearing a few days after the peak FRP days, likely due to smoke accumulation and retrieval timing. The delay in peak CO levels was more pronounced in CrIS retrievals, appearing 1-2 days later than TROPOMI's, likely associated to smoke being transported towards higher altitudes as time progressed. Future work could evaluate if models driven by FRP emissions can represent this delay or not.

Validation of satellite products was accomplished through a spatiotemporal comparison with FTIR measurements from TCCON and NDACC. Most sites demonstrated strong agreement, as indicated by NMBs and NMEs typically falling below 24% and 32%, respectively. This evaluation evidenced the ability of TROPOMI to effectively capture the majority of the CO column, particularly close to the ground when comparing such retrieval to CrIS, which reported lower column concentrations due to being less sensitive at lower altitudes. Although the satellites were successful in detecting changes in CO columns at Pasadena, they were biased low, which is in line with previous research (Sha et al. 2021). Due to limited ground-based data due to the nearby Bobcat fire and COVID-19 restrictions, validation was difficult between September 9 and 22 over Pasadena. Despite these obstacles, satellites continued to collect critical data.

Evaluation using balloon-borne measurements during a lofted smoke plume confirmed consistency between TROPOMI and CrIS CO columns for lofted plumes. However, analysis of CrIS retrieved vertical profiles and those derived from balloon-borne measurements after applying CrIS averaging kernels showed inconsistencies, with a tendency of CrIS to place plumes at lower altitudes. This suggests challenges in accurate vertical layer placement, although the overall column enhancement is captured. As TROPOMI captures the entire column, using a ratio of CrIS to TROPOMI columns might more effectively determine vertical placement.

The assessment of accuracy and differences among satellite CO products provides valuable information that contributes to the advancement of applications. In this study, the observed discrepancies in sensitivity lay the groundwork for further investigations using multi-satellite synergies to evaluate air quality models beyond just CO, but extending it to other compounds

present in smoke. Examining the vertical placement of plumes is crucial, as it plays a significant role in the accurate estimation smoke impacts. Previous research has already highlighted the substantial uncertainties in models resulting from inaccuracies in estimating injection height (Thapa et al. 2022) and smoke thickness (Ye et al. 2022), underscoring the necessity for comprehensive studies utilizing multiple satellite datasets. In light of the results of the present study, additional investigation that involves comparisons between the vertical placement information and additional measurements, such as TROPOMI aerosol layer height data, smoke height data obtained from airborne field campaigns, and active satellite retrievals like CALIPSO, has the potential to improve the precision of vertical estimations. This study also establishes the basis for evaluating the potential of synergistic utilization of CrIS and TROPOMI in estimating CO concentrations in the lower troposphere, creating a capability that neither instrument can achieve independently. TROPOMI and CrIS embody the actual essence of synergy, as they demonstrate the ability to generate a combined outcome that exceeds the sum of their individual parts.

Chapter 3 Contributions of 2020 wildfires to western U.S. air pollution

3.1 Abstract

The 2020 wildfire season had devastating consequences for infrastructure, ecosystems, and public health across the western U.S. Smoke produces particulate matter (PM_{2.5}; particles smaller than 2.5 μm in diameter) that may present heightened health risks compared to other sources of PM_{2.5}. We used the GEOS-Chem atmospheric chemical transport model coupled with a satellite-derived fire emissions inventory to evaluate the concentrations attributable to fires in the western U.S. in 2020, compared to the previous five years. Our research found that including GFAS was crucial for accurately assessing the impact of wildfires through validation with data from the AQS and IMPROVE databases. We found enhanced correlation in Washington and Montana showing high R² values of 0.63 and 0.45, respectively, in the AQS data analysis. Bias analysis indicated a neutral model performance for PM_{2.5} concentrations under 25 μg/m³, while higher concentrations saw reduced bias with fire data inclusion. For the IMPROVE dataset, the model correlations were notable in Washington, Oregon, and Montana, with R² values of 0.57, 0.48, and 0.42, respectively, and the model's bias decreased for larger PM_{2.5} concentrations. The 2020 fires emitted 328 million tons of PM_{2.5} across the western U.S., which is equivalent to the total emissions of the previous three years combined. California's case stood out as it contributed to 18% of the total emissions released by all the Western states combined over the six-year period, with this amount being produced solely in 2020. Our analysis revealed that in 2020, certain areas witnessed more than 40 days where the levels of pollutants surpassed the 24-hour air quality limit of 35 μg/m³ set by the EPA. This threshold represents the regulatory limit set by the EPA serving as a standard to assess and regulate air quality and protect public health. Cumulatively,

the western U.S. saw exposure levels of 492 million person-days in 2020, where exposure is defined as the days when a cell was above $35 \mu\text{g}/\text{m}^3$ of $\text{PM}^{2.5}$. The term 'persons' represents the cumulative number of individuals affected within the areas covered by these cells.

The year 2020 emerged as an extraordinary period in terms of air quality, with combined exposure to fire-related $\text{PM}^{2.5}$ concentrations surpassing the total exposure of the previous five years. Our study indicates that the frequency and geographical spread of days exceeding the EPA's air quality thresholds were greater in 2020 than in prior years, particularly in the western U.S., where some regions endured unhealthy air quality levels for over 40 days. This unprecedented situation highlights the importance of implementing measures to protect communities from exposure, particularly in light of the events of the past six years.

Keywords: Wildfires, air pollution, exposure, smoke.

3.2 Introduction

The 2020 wildfire season in the western U.S. damaged over 10,000 structures and endangered nearby communities (National Interagency Fire Center 2020). Approximately 4.2 million acres were burned in California over the course of 2020 Field (Cal Fire 2023), along with 1.1 million acres and .84 million acres burned in Oregon and Washington, respectively (Northwest Interagency Coordination Center 2021). The complex wildfires that formed in 2020 surpassed the previous largest wildfire events of 2017 and 2018 (Masri et al. 2021). In California, the fires claimed the lives of 91 people (Stephens et al. 2021) and exposed millions of people to degraded air quality (Higuera and Abatzoglou 2021). During periods of peak fire activity in Oregon, Washington, and California, PM_{2.5} levels on wildfire days surpassed those on days without wildfires by a factor of five (Zhou et al. 2021). Certain counties in these three states witnessed exceptionally elevated PM_{2.5} concentrations during wildfires. For example, between September 14 and September 17, 2020, Mono County in California observed consecutive days with PM_{2.5} concentrations surpassing 500 µg/m³ (Zhou et al. 2021). To very high and high concentrations are defined as annual average PM_{2.5} concentrations exceeding 25 and 10 µg/m³, respectively (Lim et al. 2020). Thus, levels exceeding 500 µg/m³ during wildfires are significantly higher and represent a severe pollution event with heightened health risks.

Western U.S. wildfires have been increasing in frequency and size. A study revealed compelling evidence that fire events in regions of the United States during the 2000s were up to four times the size, triple the frequency, and more widespread compared to the previous two decades (Iglesias, Balch, and Travis 2022). The increase in frequency and size of fires is due to several factors, including drought conditions, changes in land use (Kumar et al. 2022), and fire management techniques (Romero-Lankao and Smith 2014). For instance, in 2015, during an extreme drought year (Marlier et al. 2017), 688,000 hectares burned in Oregon and Washington, while wildfires consumed over 3.6 million hectares in the western United States. Among the major causes of the 2020 wildfire events was the abnormally prolonged and severe drought that occurred in the region starting from 2012 (Keeley and Syphard 2021). The drought was one of the most severe in the region, starting in 2012 and lasting 3–5 years in California (Robeson 2015; Jacobsen and Pratt 2018).

In 2020, five of the six most significant events occurred within a span of two months, specifically in August and September. A study tracing back to 1860 revealed that since 2000, California has witnessed eighteen of the twenty most devastating fires in terms of both casualties and property damage. (Cal Fire 2023; Keeley and Syphard 2021). Larger wildfires will continue to catalyze ecosystem changes, changing climate, and exposing populations to its emissions (Coop et al., 2020). As wildfire trends continue to evolve, regions previously unaffected by severe smoke pollution might begin to face such conditions (Marlier et al. 2022).

In addition to consequences for atmospheric greenhouse gas concentrations (Jerrett, Jina, and Marlier 2022) and natural ecosystems (Albery et al. 2021; Roces-Díaz et al. 2022; Halofsky, Peterson, and Harvey 2020), fires also contribute to trace gas and aerosol concentrations (Andreae 2019; Voulgarakis and Field 2015). In the western U.S., wildfires have reversed decades of improvement in other air pollution sources (McClure and Jaffe, other citations). Fine particulate matter (PM_{2.5}; particles smaller than 2.5 microns) can adversely impact human health. In particular, high levels of PM_{2.5} can irritate the lungs, weaken immune function, and increase susceptibility to respiratory infections due to exposure (Thangavel, Park, and Lee 2022). Exposure to fire-specific PM_{2.5} (“smoke PM_{2.5}”) has been linked to the worsening of asthma, chronic obstructive pulmonary disease, cardiovascular disease, and an increased risk of mortality (Jia Coco Liu et al. 2016; Reid et al. 2016). Vulnerable groups are more prone to develop respiratory and cardiovascular disorders due to PM_{2.5} exposure from wildfires. The elderly, children, and those living in poverty, will be most sensitive to the risks associated with PM_{2.5} exposure from wildfires (Delfino et al. 2009; Sutherland et al. 2005; Youssouf et al. 2014). These groups can exhibit increased vulnerability due to preexisting health conditions, particularly among those aged 65–99 years (Delfino et al. 2009). Additionally, smaller airways, especially in young children (0–4 years), play a significant role in heightening susceptibility and leading to increased respiratory admissions during wildfires. Individuals with lower socioeconomic status may also encounter additional challenges when adapting to wildfire smoke exposure (Liu et al. 2017).

Smoke from wildfires produces particulate matter that may possess greater health risks than equivalent doses of PM_{2.5} from the ambient. (Kim et al. 2018; Wegesser, Pinkerton, and Last

2009; Aguilera et al. 2021). This increased toxicity can be attributed to factors like inflammation and altered pulmonary activity (Migliaccio et al. 2013). Wildfire PM_{2.5} may be more toxic because of a highly carbonaceous composition (Adetona et al. 2016; Wu, Jin, and Carlsten 2018) or to higher concentration of polar organic compounds (Verma et al. 2009), which can lead to enhanced lung inflammation and oxidative stress compared to urban particles (Karthikeyan, Balasubramanian, and Iouri 2006; Williams, Franzi, and Last 2013; Aguilera et al. 2021). Furthermore, wildfire smoke can cover vast distances and go beyond geographical borders., meaning that even populations in areas without active fires can experience smoke-related effects (Black et al. 2017). Thus, estimating PM_{2.5} concentrations in unmonitored areas and distinguishing between wildfire and non-wildfire PM_{2.5} is imperative for accurate public health assessments.

Current methodologies for estimating PM_{2.5} concentrations in unmonitored areas typically involve the use of extensive data and computationally intensive modeling techniques and may face challenges in distinguishing fire-specific PM_{2.5} from other sources, such as traffic and industrial emissions Field (Aguilera et al.,(Aguilera et al. 2023). Numerous techniques have been documented to estimate PM_{2.5} in unmonitored regions and to estimate fire-specific emissions. For instance, statistical methods have been used to isolate wildfire-specific PM_{2.5} from other sources of emissions (Aguilera et al. 2023). Other studies have implemented regression analyses (Hoek et al. 2008) and machine learning for predicting PM_{2.5} fluctuations (Di et al. 2019; Reid et al. 2021; Childs et al. 2022; Reid et al. 2015). Alternative approaches have combined traditional data (Cleland et al. 2020) and amalgamated traditional and untraditional information, such as data from private pollution sensors, mobile devices, social media insights, and internet activity

(Burke et al. 2022). Other approaches have utilized remotely-sensed information (Al-Hamdan et al. 2014) and chemical transport models (Zhang et al. 2020; Jia Coco Liu et al. 2017).

Prior research examining the 2020 wildfires has identified significant surges in PM_{2.5} emissions Field (Albores et al.,(Albores et al. 2023). These findings have been reinforced, suggesting that the wildfires intensified the effects of short-term PM_{2.5} exposure (Zhou et al. 2021). Yet, when it comes to the detailed examination of the fire-specific contribution to PM_{2.5} pollution in the western U.S. from 2006 to 2020, comprehensive studies, remain scarce (Aguilera et al. 2023). While previous studies have laid important groundwork, significant gaps remain in model-based fire-specific research. Research using modeling has provided estimates of fire-specific PM_{2.5} concentrations in the Western U.S. between 2004 and 2009, identifying an impact on an estimated 46 million people (Liu et al. 2017). However, these studies highlighted areas for improvement, such as the inclusion of daily AQS validation and comprehensive exposure assessments. Additionally, while some studies have aimed at enhancing model outputs, they often omitted important ground-based rural datasets like IMPROVE (Zhang et al. 2020). Contrastingly, other research utilized coarser Geos-Chem models, refining them with monitoring station data (Zhang et al. 2023), a method that differs from our nested model simulation approach. Our research is designed to address these gaps by providing a comprehensive analysis of 2020's fire-specific PM_{2.5} emissions. We extend our analysis to a more recent timeframe (2015-2020), covering the broader western U.S. region with a nested grid simulation that includes validation data for both rural and urban areas. Our study aims to enrich the understanding of the broader implications of wildfires on air quality, addressing the

shortcomings of contemporary studies in quantifying the extensive impact of fire-specific PM_{2.5} emissions.

We use the GEOS-Chem chemical transport model to examine the influence of western U.S. fires on air quality from 2015 to 2020. Our research aimed to answer three questions. First, what is the significance of the 2020 wildfire season in comparison to the previous five years? Second, what discrepancies exist between modeled data and monitoring stations, highlighting the impact of GFAS inclusion? And third, to what extent was the population affected by high levels of PM_{2.5} caused by the wildfires? Our study measures the frequency and geographic range of days exceeding EPA air quality thresholds, particularly in the western US, aiming to provide insights on exposure to help mitigate risks under future extreme events, like the 2020 wildfires.

3.3 Data and Methods

3.3.1 GEOS-Chem Configuration

We use the GEOS-Chem chemical transport model v12.7.0 to perform a nested grid simulation across western North America at $0.25^\circ \times 0.3125^\circ$ resolution from 2015-2020, covering a longitude range from -126 to -99.75 degrees and a latitude range from 30 to 51 degrees. We conducted an aerosol-only simulation, which utilizes stored monthly average concentrations of OH, NO₃, O₃, and total nitrate from a prior full-chemistry simulation as well as production and loss rates for H₂O₂. Following a one-year model spin up, we first simulated global boundary conditions at a $4^\circ \times 5^\circ$ resolution for 72 vertical levels before running the nested grid simulations.

Global inventories, ship emissions, dust, and sea salt retrievals were used as inputs in the GEOS-Chem model run, while keeping anthropogenic emissions constant over time. This approach also involved processing a variety of data files and inventories to accurately simulate atmospheric conditions. The model utilized data from multiple sources, such as NH₃ sources, as well as aerosol and chemical components like PM_{2.5} and DMS, along with lightning data. Our approach was configured in agreement on previous studies that estimated PM_{2.5} using offline aerosol data (Marvin et al. 2023). Modifications were made to allow the use of the version v12.7.0 of Geoschem as recommended by Melissa Sulprizio and Robert Yantosca (<https://github.com/geoschem/geos-chem>).

Several satellite-based fire emissions inventories are available at global scales (T. Liu et al. 2020). These inventories use different approaches to estimate fire emissions, including the "bottom-up" approach based on burned area and the "top-down" approach based on fire radiative power (T. Liu et al. 2020). In this study, we used the GFAS top-down fire emissions inventory available at 0.1° × 0.1° resolution. GFAS has several benefits over other fire emissions inventories. It is available without an extended lag time, includes plume injection heights (Rémy et al. 2017), and has performed well in prior modeling simulation studies in the western U.S. (Carter et al. 2020) GFAS uses satellite-based Fire Radiative Power (FRP) retrievals from the MODIS instruments onboard the Terra and Aqua satellites (Kaiser et al. 2012). It converts FRP observations from MODIS instruments into fuel consumption using a linear relationship (Kaufman et al. 2003). Emissions are then derived using land-use-dependent conversion factors. GFAS uses MODIS aerosol optical depth (AOD) to determine scaling factors for emissions of OC, BC, PM_{2.5}, and other species. It corrects for cloud cover gaps and filters spurious FRP

observations of volcanoes, gas flares, and other industrial activity (Kaiser et al. 2012). Since the previously mentioned factors can lead to missing data, GFAS employs a method called persistence to fill in these gaps. This involves using the previous day's observed FRP values until new data is available. However, this approach might result in an overestimation of fire duration. Such overestimation is particularly evident in areas frequently covered by clouds or where the variability of fires over time is significant (Di Giuseppe et al. 2018; Kaiser et al. 2012).

We perform two model simulations from 2015-2020 with and without the inclusion of fire emissions. The difference between the two simulations provides the fire-specific contribution to surface PM_{2.5}. Since Goes-Chem does not produce PM_{2.5} concentrations as a direct output, we obtained PM_{2.5} by summing selected components of an aerosol simulation as described in Equation 1. We use surface modelling estimates in the first three-dimensional level as the input to our measurements.

Equation 1 displays the components of our PM_{2.5} estimation. NH₄ refers to ammonia; NIT to Inorganic nitrates; SO₄ to Sulfate; BCPO refers to Hydrophobic black carbon aerosol; BCPI refers to Hydrophilic black carbon aerosol; OCPO to Hydrophilic organic carbon aerosol; OCPI to Hydrophilic organic carbon aerosol; DST1 to Dust aerosol, Reff = 0.7 microns; DST2 to Dust aerosol, Reff = 1.4 microns; SALA to Fine (0.01-0.05 microns) sea salt aerosol. (K.E. Knowland, C.A. Keller, and R. Lucchesi 2020)

$$\text{PM2.5} = \text{NH4} + \text{NIT} + \text{SO4} + \text{BCPO} + \text{BCPI} + \text{OCPO} + \text{OCPI} + \text{DST1} + \text{DST2} + \text{SALA}$$

3.3.2 Observational Datasets Used for Model Validation

We compare simulated PM_{2.5} to surface-level station measurements derived from the Air Quality System (AQS) and the Interagency Monitoring of Protected Visual Environments database (IMPROVE) network. The AQS data reports daily 24-hour average PM_{2.5} concentrations across

Western US states. Since the AQS measurements provide limited data in rural areas, thus, we include stations from the IMPROVE network. This network provides information in remote areas, with measurements every three days. Although IMPROVE sites employ a filter-based method like the Federal Reference Method (FRM) for measuring PM_{2.5} mass concentrations, it's important to note that their data is generated at a lower temporal resolution, with measurements available only every three days. This data collection approach, while valuable, introduces some uncertainties into the dataset. These uncertainties, coupled with the less frequent data updates, can affect the accuracy and timeliness of PM_{2.5} concentration information when compared to data obtained from AQS. Nonetheless, these sites fill in spatial gaps that the AQS system (Gantt et al. 2020).

We filter AQS and IMPROVE sites that were present throughout the entire six-year at least 50% of days during the fire season (May 1 to November 1). The extensive time frame chosen for the season's definition was shaped by the exceptionally active and long-lasting 2020 fire season in California. This season, considered one of the most destructive on record, began early in April and extended late into November (Cal Fire 2023). To compare surface-level station measurements against our simulated PM_{2.5} concentrations, we match measurements of the stations with the grid cells that correspond spatially and temporally in our modeled data and average data from multiple stations within the same GEOS-Chem grid cell. Geos-Chem was validated against both datasets, with AQS providing daily measurements and IMPROVE data collected every three days. Since station measurements include all emissions sources, we compare to the all-source PM_{2.5} which integrates emissions data from GFAS as well as various non-wildfire sources.

3.3.3 Population-Level Exposure

We estimate population-level exposure over the EPA's 'Unhealthy' air quality benchmark of 35 $\mu\text{g}/\text{m}^3$ (Environmental Protection Agency 2016) using 2020 population estimates derived from the Gridded Population of the World (GPW v4) database (Center For International Earth Science Information Network-CIESIN-Columbia University 2018). This database uses the areal-weighting method to disperse non-spatial population figures onto individual grid cells based on geospatial administrative boundary data at a resolution of 30 arc-seconds (Lloyd, Sorichetta, and Tatem 2017). We calculate the number of "person-days," which represents the product of the number of individuals exposed to concentrations meeting or exceeding this threshold daily within each grid cell. Furthermore, within these grids, we pinpointed locations where the state frequently observed daily $\text{PM}_{2.5}$ concentrations exceeding 35 $\mu\text{g}/\text{m}^3$, highlighting the most affected areas during our observation period.

3.4 Results

3.4.1 Fire emissions

As expected, $\text{PM}_{2.5}$ fire emissions were at least 189.7 Million Tons higher in 2020 than in the previous five years (Table 5). With daily concentrations averaging above 70 $\mu\text{g}/\text{m}^3$, the 2020 levels exceeded the previous high average daily peaks observed during the fire season of 2017, which were around 51 $\mu\text{g}/\text{m}^3$ (Figure B2). Compared to the 2015-2019 period, 2020 had higher fire activity in Arizona, Oregon, Colorado, Wyoming, and California (Table 5). Furthermore, we observe that major anomalies occur across the coastal states (Figure 5).

Table 5: summarizes annual fire emissions at the state level (see Table B1 for percentage contributions). Total 2020 emissions in the western US were 328 Million tons of PM2.5 which represents about 57% of the emissions released from 2015-2019. The emissions generated in 2020 were equivalent in magnitude to the three years preceding that year. In California and Colorado, 2020 PM2.5 emissions were 162.7, and 59.6 Million Tonnes, respectively, which was higher than the sum of the five precedent years (157.8 and 23.0 million Tonnes). In California, the 2020 emissions constituted 18% of the total emissions released in the western U.S. over the six-year duration.

	2015	2016	2017	2018	2019	2020
<i>Arizona</i>	3.25	8.36	8.78	5.32	6.47	12.11
<i>California</i>	31.17	24.3	44.7	45.3	12.2	162.7
<i>Colorado</i>	0.91	4.3	2.2	13.8	1.8	59.7
<i>Idaho</i>	24	16.0	18.4	9.1	5.0	7.7
<i>Montana</i>	12.9	6.7	39.4	4.2	2.4	3.3
<i>Nevada</i>	0.21	1.6	4.2	9.6	0.7	3.2
<i>New Mexico</i>	0.77	3.1	1.9	4.7	1.8	4.4
<i>Oregon</i>	17.67	9.0	27.5	16.8	6.6	45.9
<i>Utah</i>	0.93	3.0	7.4	12.6	1.7	4.8
<i>Washington</i>	43.15	3.1	15.1	8.8	3.8	8.2
<i>Wyoming</i>	0.69	9.5	1.1	8.5	0.9	16.2
<i>Total</i>	135.65	88.9	170.6	138.5	43.5	328.2

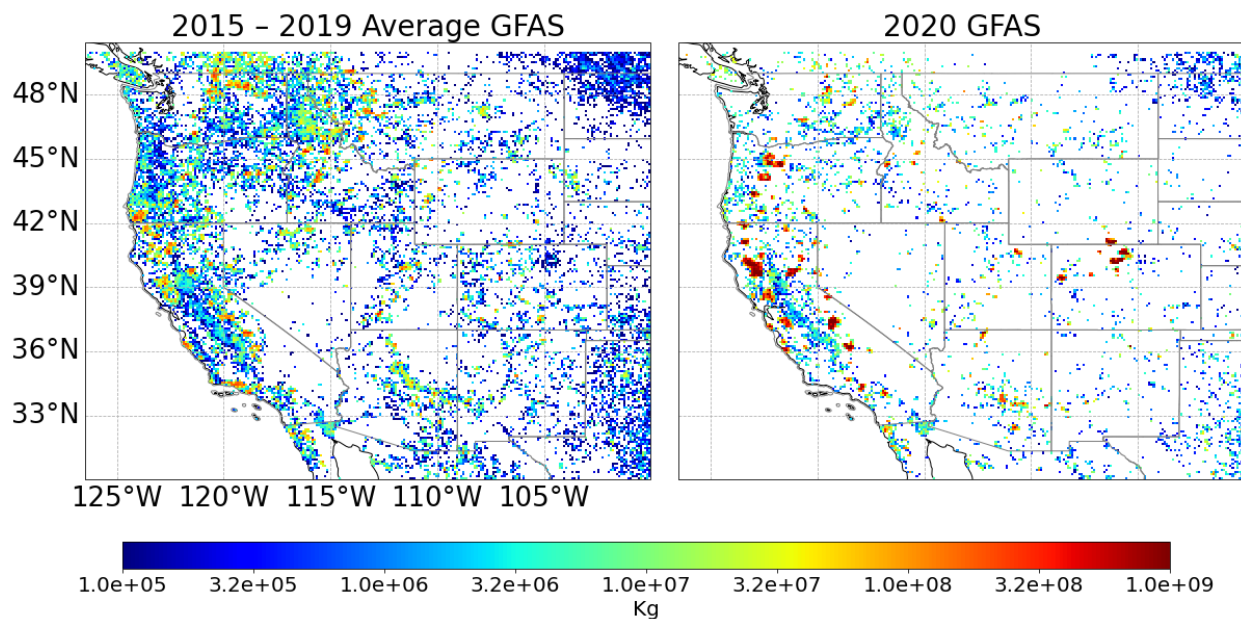


Figure 5: Annual average emissions of GFAS. The leftmost figure displays the average of the sum of all the daily emissions for each year for the years 2015-2019. Figure in the center displays the sum of all the daily emissions of 2020, and figure in the right displays the difference of both figures.

3.4.2 GEOS-Chem Simulation Results

Figure 6 shows the geographic distribution of annual average $PM_{2.5}$ concentrations based on GEOS-Chem simulations with and without the inclusion of fire emissions for the 2015 to 2019 average and 2020. The simulations without fires show similar spatial patterns and magnitude across the years, but significant discrepancies arise with the inclusion of fire emissions. Fire-specific $PM_{2.5}$ in 2015-2019 and 2020 show high concentrations of fires in the coastal areas and Colorado (2020).

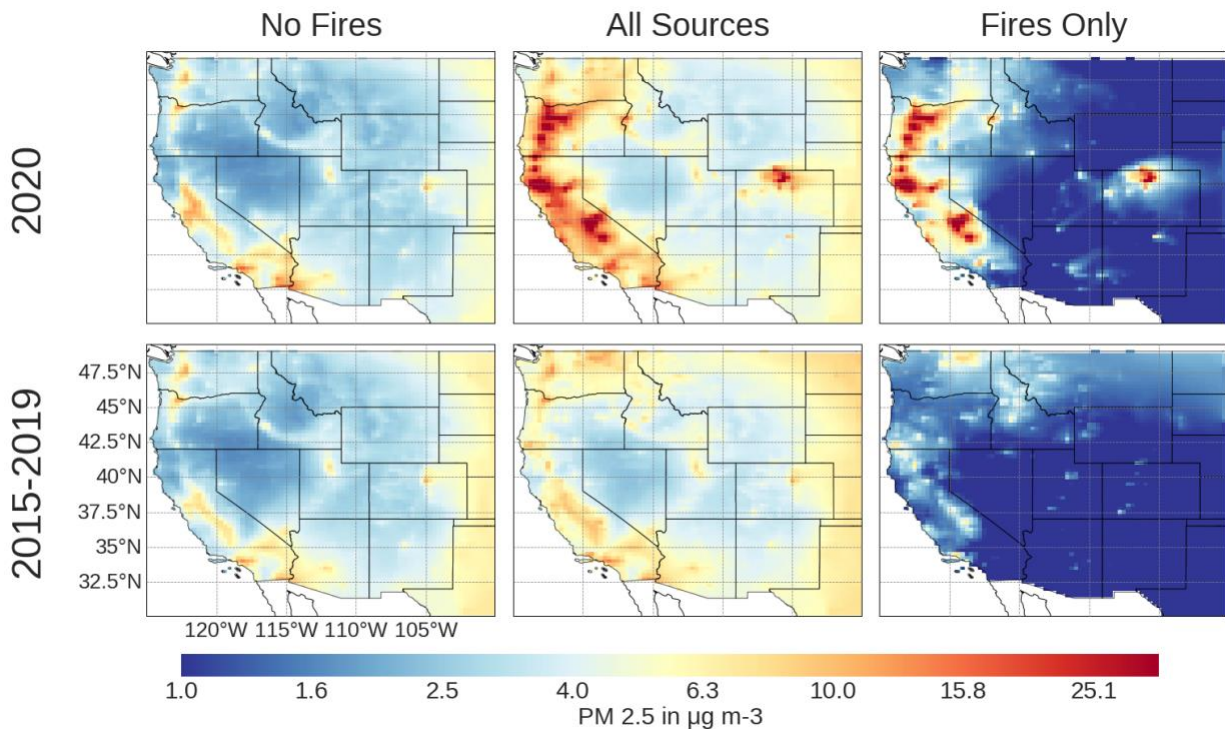


Figure 6: displays $PM_{2.5}$ concentrations product of the modeling using Geos-Chem. The upper row displays the annual average of the daily concentrations for 2020. And the lower row corresponds to the mean of the average daily concentrations estimated by GEOS-Chem. The left columns correspond to the simulation without the inclusion of the fire inventory, the center columns correspond to the concentration including the emissions of the fire inventory, and the right columns correspond to the subtraction of the modelled results using the fire inventory, minus the modelled results without the fire inventory.

3.4.3 GEOS-Chem Validation

We validate the GEOS-Chem model outputs across spatial and temporal dimensions in both urban and rural areas using the AQS and IMPROVE datasets and examine the effects of integrating wildfire data. We assess the correlation of daily averages over time for individual and aggregated stations. In our analysis, we assessed bias by comparing the GEOS-Chem model's PM_{2.5} concentrations to measurements from AQS and IMPROVE datasets; station data within the same grid cell were averaged. To quantify the bias, we subtracted the GEOS-Chem values from the measurements in both AQS and IMPROVE datasets. This approach allowed us to directly evaluate the differences between the model's predictions and the observed data, providing valuable insights into the model's performance in estimating PM_{2.5} concentrations. We note that some states have more concentrated stations than others (Table B2).

The GEOS-Chem model displays limited concurrence with AQS measurements without the inclusion of fire emissions. As shown in Figure 7, the incorporation of fire emissions improved the estimations by orders of magnitude in many locations. Correlations in coastal areas tend to be lower than inland areas, even with the inclusion of fire emissions. Figure B2 shows a time series of average daily measurements for station measurements and GEOS-Chem simulations. Fire emissions are needed to replicate the peak values in 2015, 2017, 2018, and 2020

Washington and Montana show the highest correlations across the sites in their territory, with R² coefficients of 0.63 and 0.45 respectively, with the shortcoming of having 12 and 13 stations respectively (Table B2). We also find that California, where most fires occurred, displayed an

average $R^2 > 0.21$ (Table B2) across all stations and all years, for All-Source concentrations relative to the 65 AQS stations that were matched to the GEOS-Chem simulations.

In Figure 8, we estimate the bias of our modelled concentrations with and without fire emissions relative to AQS measurements. We organize the data into subgroups based on observed $PM_{2.5}$ concentrations, following previous approaches (Wilkins et al. 2018). The data indicates that at concentrations lower than $<25 \mu\text{g}/\text{m}^3$, both datasets exhibit a neutral bias. However, at concentrations exceeding $25 \mu\text{g}/\text{m}^3$, the inclusion of fire emissions leads to a reduction in bias. It is important to mention that Figure 8 displays the effect of biases without accounting for outliers below and above the first and third percentile. Interestingly, in 2020, there were few days where measurements larger than $>150 \mu\text{g}/\text{m}^3$ were observed (Figure B4).

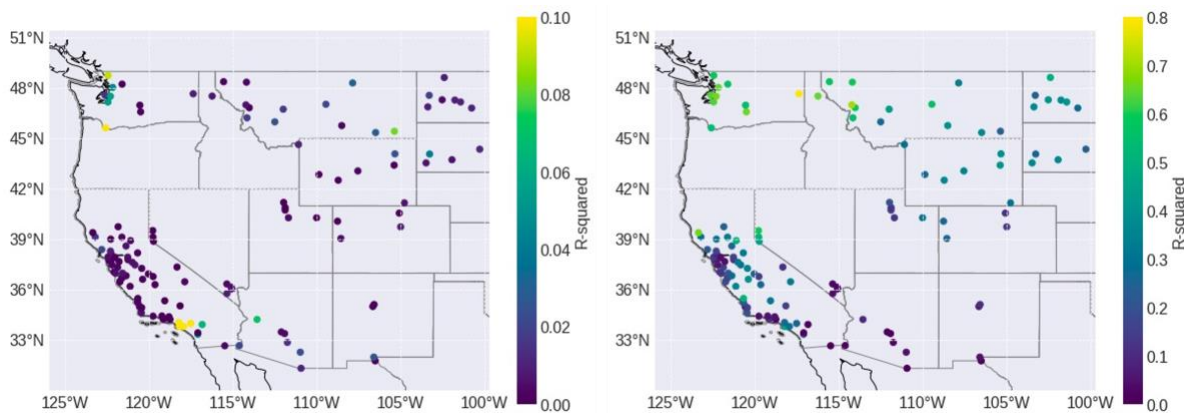


Figure 7: Correlation of 2015-2020 daily concentrations for each of the AQS monitoring stations when compared to GEOS-Chem. This figure showcases the location of each of the AQS stations analyzed in this study, and colors representing each of the locations with the R^2 value corresponding to the correlation of the daily measurements of the station that correspond in space and time to the measurements from the model for the fire season between April 1st, and November 1st. We filter to locations that existed across the 6 years of study, and that had at least 50% of the measurements for date period in each year.

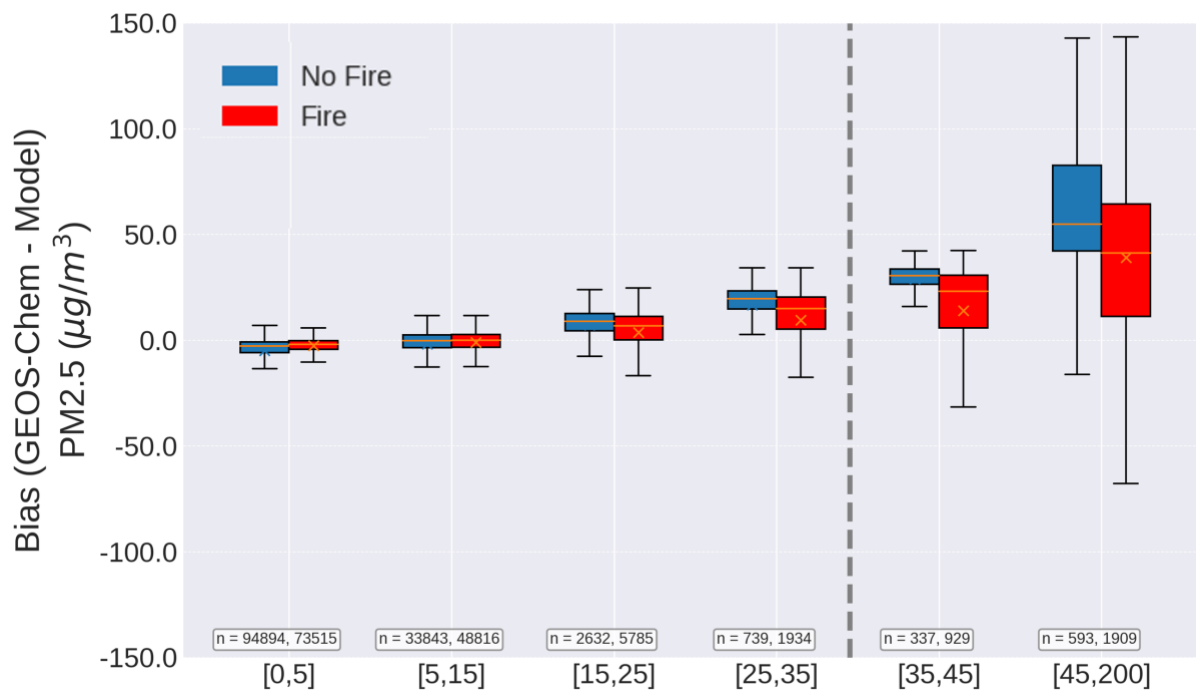


Figure 8: This figure showcases the bias estimation of the modelled PM_{2.5} concentrations relative to the AQS station measurements for model runs with and without the inclusion of the GFAS inventory. The measurements are sub grouped by particle size.

We also compare the modelled PM_{2.5} with the IMPROVE stations. Similar to AQS, Figure 5 shows that considering all sources improves model estimation correlation coefficients with station measurements from IMPROVE. To conduct a comparison between IMPROVE and Geos-Chem, the model was sampled at a 3-day interval, aligning with the temporal frequency of IMPROVE measurements. IMPROVE stations provide better spatial coverage in rural areas, allowing insights in some areas more affected by fires. We find there is a notable correlation between R² values and the states of Washington, Oregon, and Montana, these states demonstrate the strongest correlations with R² values of 0.57, 0.48, and 0.42, respectively (Table B4). Interestingly, the observed correlations between the states of Washington and Oregon and the Air Quality System (AQS) are comparable.

When comparing GEOS-Chem concentrations and IMPROVE data, we see a decrease in bias for larger concentrations (Figure 10) compared to AQS data (Figure 8). This supports the idea that trends at IMPROVE sites tend to correlate better in wildfire-prone areas due to the proximity to fires in rural locations and the smaller contribution of background PM_{2.5} sources (McClure and Jaffe 2018).

Upon analyzing a time-series and comparing its measurements over the years, an interesting pattern was observed, as depicted in Figure B4. The inclusion of all sources simulated concentrations tends to be much larger than the emissions observed by the stations during the peak of the fires. In September 2020, the all-sources model overestimated station measurements by 60 ug/m³, which contrasted with the comparison of All-Sources modeled concentration versus AQS data. A possible explanation of this issue could be the use of persistence when FRP data was not available during GFAS estimations, due to very thick smoke (Ye et al. 2022).

The significance of using fire inventories in rural areas is demonstrated in Figure B5. It is noticeable that when the GFAS inventory was included, R² improved from 0 to 0.21, which contrasts with Figure B3, where we saw an increase in R² from 0.12 to 0.47 when comparing AQS data with Geos-Chem.

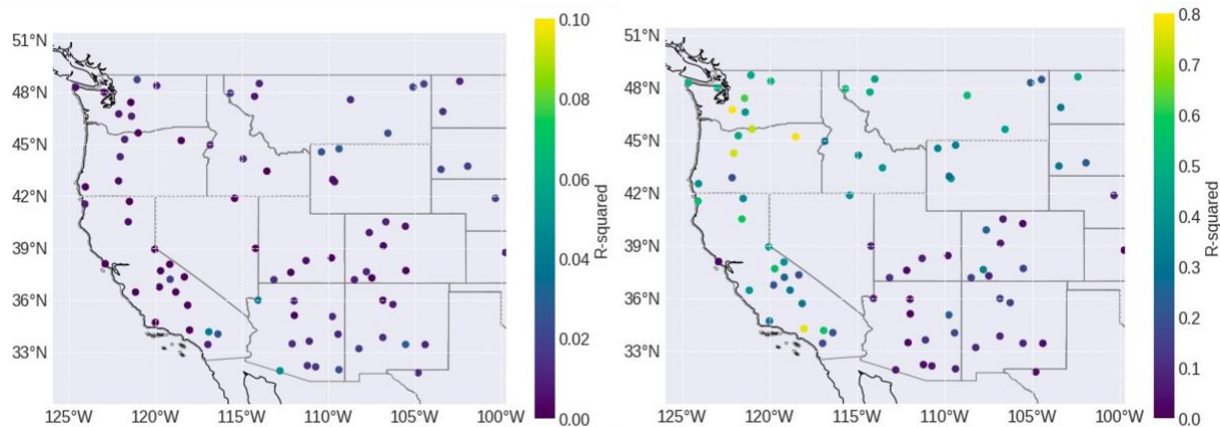


Figure 9: Correlation of 2015-2020 third-day concentrations for each of the IMPROVE monitoring stations when compared to GEOS-Chem. This figure showcases the location of each of the IMPROVE stations analyzed in this study, and colors each of the locations with the R^2 value corresponding to the correlation of the third-day measurements of the station that correspond in space and time to the measurements from the model for the fire season between April 1st, and November 1st. We filter to locations that existed across the 6 years of study, and that had at least 50% of the measurements for date period in each year.

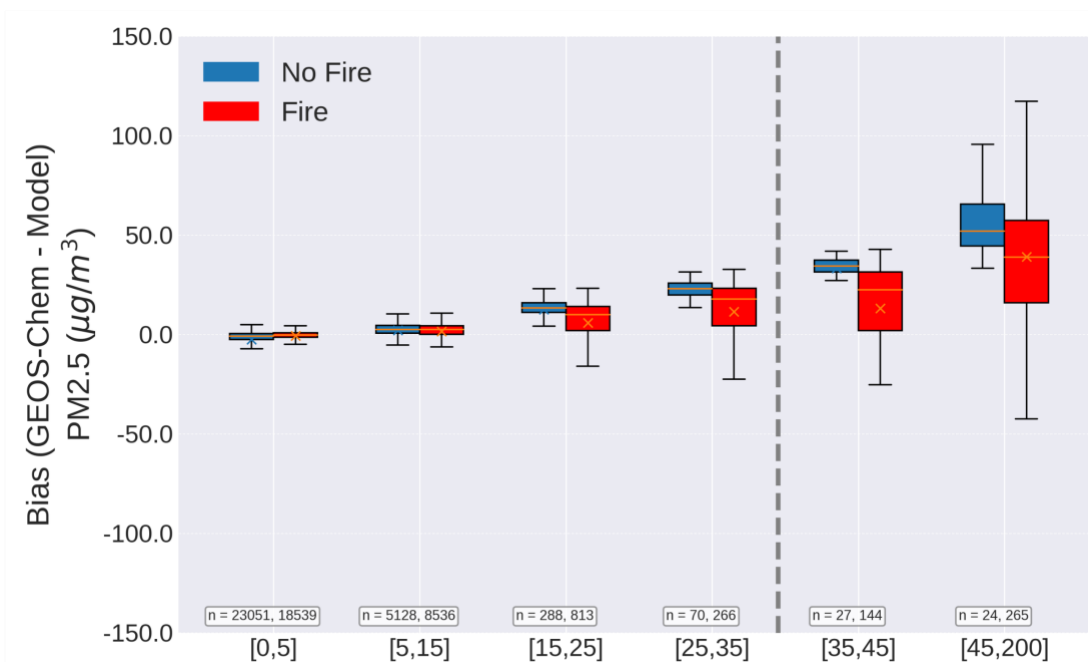


Figure 10: Showcases the bias estimation of the modeled $PM_{2.5}$ concentrations relative to the IMPROVE station 3-day measurements for model runs with and without the inclusion of the GFAS inventory. The measurements are sub grouped by particle size.

3.4.4 Population exposure

We estimate population exposure using the concentrations of fire-specific PM_{2.5}, thus minimizing the potential for exposure misclassification bias which refers to the difficulty in discerning between emissions that come from a fire versus emissions that come from any other source in the background (Jia C. Liu et al. 2015; Lassman et al. 2017). We assess the number of days that exceed the EPA's designated benchmark for 'Unhealthy Air Quality' to map the distribution of days that exceeded the threshold for the six-year period (Figure 11). We found that the western U.S., particularly California, had the largest area of exceedances over this threshold attributable to fires. The product of the number of days and area exceeding this threshold was higher in 2020 than any prior year, and was 1.74 times higher than the second largest year (2017) (Table B3). In 2020, the contribution of wildfires only exceeded the EPA threshold for over 40 days in various regions.

We estimate the number of days that populations in the western U.S. were exposed to PM_{2.5} above the 35 ug/m³ unhealthy air quality threshold (Table 6). California, which has the largest population and was most affected by fire pollution, had 347 million person-days. This represents the same amount of exposure as all the other states combined with all the years combined between 2015 and 2020. Nevada and Colorado experienced 5.3 and 14.1 times more exposure when compared to the previous five years combined. Across the western U.S., the population exposure in person days from 2020 was 492 million person-days, which is higher than the 489.1 million of person days exposed in the prior five years combined.

Table 6: displays the person-days of exposure that each state experienced during the six-year period. To estimate such number, we use smoke-specific PM2.5 emissions, and select the grid cells that exceeded the 35 ug/m3 EPA Standard, on each day. Then we calculate the number of days that each grid-cell was above the EPA Standard for each year and multiply it times the population in each of the grid cells. We then organize it by state. State area and population influence these results so it is recommended to consider table B5 in the appendix which includes population and area for each state.

	2015	2016	2017	2018	2019	2020
California	16.0	35.4	59.7	140.0	8.3	347.2
Oregon	4.8	0.8	16.7	15.9	2.4	27.0
Washington	19.7	0.6	60.7	50.7	1.4	51.7
Idaho	6.0	5.4	8.3	3.3	0.8	8.0
Montana	5.0	0.6	5.5	3.4	0.1	2.6
Wyoming	0.3	0.2	0.1	0.5	0.0	0.6
Nevada	0.8	0.2	0.5	1.2	0.1	14.8
Utah	0.0	0.3	1.1	8.3	0.0	0.8
Colorado	0.1	0.1	0.4	2.1	0.1	39.0
New Mexico	0.0	0.4	0.0	0.2	0.0	0.1
Arizona	0.1	0.2	0.4	0.1	0.4	0.5
Total	52.7	43.9	153.3	225.6	13.6	492.0

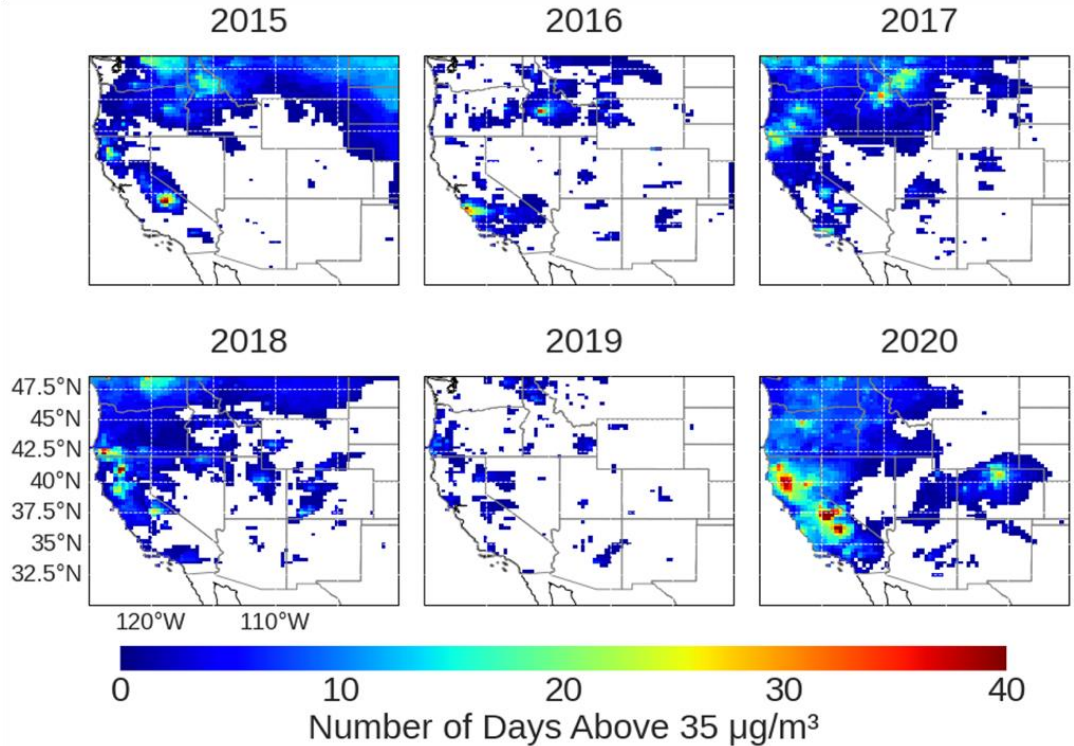


Figure 11: Map of the distribution of days that exceeded the EPA Standard. This figure displays the locations in the Western US that exceeded the EPA Standard of $35 \mu\text{g}/\text{m}^3$. The color of each location refers to the number of days that each site was above the EPA standard on a given year.

3.5 Discussion

3.5.1 Summary of Results

The level of $\text{PM}_{2.5}$ fire emissions in 2020 exceeded the levels observed in the last five years. The primary cause for this was wildfires. However, it is important to note that GFAS, which was used in the analysis, does not differentiate between wildfires and other types of fires, such as prescribed burns or agricultural burning. Across the western U.S., this amounted to 328 million tons, which is equivalent to the combined emissions of the three preceding years. The states of Oregon and California were particularly affected. For instance, California's emissions in 2020 accounted for 18% of the total emissions of all the states in the western U.S. over a six-year period.

When comparing modeled PM_{2.5} concentrations with and without fire emissions, a significant difference emerges, highlighting the relevance of fires. Incorporating fire emissions into the model proved crucial to achieve greater accuracy across various sites. The reason why there are discrepancies between the model and observations is that there are multiple sources of data that are not accounted for, especially in rural areas where other emission inventories are harder to retrieve. This is especially important for rural areas, as we found significant differences in correlation coefficients when comparing our No Fire and All Source results to AQS and IMPROVE, highlighting the need for improved data inputs in these regions.

Given the relevance of the 2020 fire season, it is critical to use fire inventories to understand exposure patterns so health implications and broader societal impacts of wildfires can be assessed. This study shows that in 2020, the number of days and locations that exceeded the EPA's designated threshold surpassed previous years in many locations in the western U.S., with some regions experiencing unhealthy air quality levels for more than 40 days. California, for example, had 347 million person-days of exposure over the 35 µg/m³ threshold in 2020. This figure is record-breaking as it represents the total exposure of all western states together from 2015 to 2020. Taken together, the western U.S. registered an exposure of 492 million person-days in 2020, slightly edging out the total of 489.1 million person-days of exposure over the preceding five years.

3.5.2 Limitations

This study has identified several sources of uncertainty, which may present opportunities for future research. The first set of uncertainties pertains to PM_{2.5} estimation, the second set to validation, and the third set to exposure. Firstly, there are uncertainties regarding the way PM_{2.5} emissions were calculated. One challenge of using GFAS as an input to GEOS-Chem is its potential inability to comprehensively capture fire emissions, especially in areas with dense smoke (Ye et al. 2022). There is a tangible risk that satellite algorithms may misinterpret extremely dense plumes as cloud cover. It's important to note that this study is based on the GEOS-Chem model v12.7.0, which, despite being generally reliable, has certain biases and limitations. Due to conducting an aerosol-only run, reliance on archived mean output may create biases. Furthermore, uncertainties in factors such as wildfire plume transport can further impact the accuracy of our estimates of state-level pollution.

Second, our validation approach could create uncertainties because GEOS-Chem output cells are relatively coarse when compared to the station point location. This could pose challenges during the process of matching station data. Because averaging was applied to sites located within the same grid cell, a potential source bias may be introduced. Furthermore, uncertainty could be introduced due to the rigorous filtering of AQS and IMPROVE data, particularly our stringent criteria, which included a focus on common stations over a six-year span and the requirement for at least 50% data coverage during the fire season. This threshold was chosen based on 183 days for AQS and 60 days for IMPROVE, considering sites available for the entire six years. Consequently, if there was a site with less than 50% data coverage in one of the years, it would

have been excluded from the analysis over the six-year period. There might also be issues with the use of the IMPROVE network data due to its lower temporal resolution.

Thirdly, there may be uncertainties regarding exposure estimates. Challenges may arise from the regridding of cells during interpolation processes. Moreover, it should be noted that the GPW v4 database utilizes administrative boundaries as a basis for estimating population figures which may result in disregarding micro-level population distributions which could be particularly relevant at relatively coarse GEOS-Chem grid cell interpolations. Lastly, the use the current 'Unhealthy' benchmark might not perfectly encapsulate health risks across diverse populations.

3.5.3 Implications and future work

The research findings highlight the significance of fire inventories in climate models. However, addressing the uncertainties in these models necessitates enhancing the accuracy of these inventories. One way to achieve this is by improving the accuracy of top-down retrievals through better satellite sensors and through more accurate algorithms, which could be particularly biased during large combustion events like wildfires.

To attain better models, superior instruments are needed to validate our measurements. Therein lies an opportunity to implement regulatory quality sensors, especially in remote locations. This study also emphasizes the need to increase the frequency of IMPROVE measurements and the spatial distribution of such retrievals.

Another important interrogative that comes out of this research is whether exposure disproportionately affected vulnerable populations more than other groups, particularly those who spend their time outdoors or those who face difficulties in adapting to wildfire smoke exposure due to their socioeconomic disadvantage. For instance, it has been documented that agricultural regions in the Central Valley and Central Coast may be highly vulnerable to future increases in fire-specific PM_{2.5} concentrations (Marlier et al. 2022). Similarly, socioeconomic disparities can make a significant difference in how individuals experience and respond to wildfire-related pollution (Liu et al. 2017). The potential environmental justice implications of wildfire-related pollution are evident in the disparities in both exposure and adaptation.

3.6 Conclusions

This study critically examines the 2020 wildfires that occurred in the western United States, highlighting their unprecedented impact compared to the previous five years. In 2020, the exposure to fire-specific PM_{2.5} concentrations significantly exceeded that of the prior five years combined. Our research utilized the GFAS inventory, which played an essential role in accurately assessing the impact of wildfires. This was validated through comparison with AQS and IMPROVE databases.

In 2020, the magnitude of wildfires that occurred was unprecedented, leading to a massive emission of 328 million tons of PM_{2.5} in the western United States. This amount was equivalent to the total emissions of the previous three years, clearly highlighting the severity of the situation. California played a significant role in this, contributing to 18% of the total emissions from all western states over six years, but solely in 2020. During this year, population exposure

was also unprecedented, with some areas experiencing over 40 days when pollutant levels surpassed the EPA's 24-hour air quality limit of 35 $\mu\text{g}/\text{m}^3$.

Our study provides valuable insights into the severity of the 2020 wildfire season compared to the previous five years, and the potential health risks associated with exposure to high PM_{2.5} levels. Our findings also highlight the discrepancies between modeled and monitored data, particularly with the inclusion of GFAS. Moreover, our research emphasizes the need for precise and comprehensive data to help shape effective environmental and public health policies amidst increasing wildfire frequency and intensity. By analyzing days exceeding EPA air quality thresholds in the western U.S., we have identified vital information that can help mitigate health risks in future extreme wildfire events. Our study paves the way for future research aimed at understanding the impact of fire-specific emissions, their relevance, and how to adapt to the constantly changing climate.

4 Overarching conclusion

This dissertation provided an in-depth exploration of the 2020 wildfires in the United States, employing unique approaches using a multi-satellite synergy and a chemical transport model. These approaches were crucial in uncovering changes in atmospheric composition due to the wildfires and their impacts on population exposure.

Central to this study was the use of CrIS and TROPOMI satellite data to analyze carbon monoxide (CO) emissions. This analysis highlighted the spatial variability in CO concentrations, a discovery made possible through the synergistic application of data from both satellites. Notably, TROPOMI data indicated higher CO values near fire sources, signifying a significant contribution of surface-level concentrations to the total atmospheric CO. This finding was validated through comparisons with ground-based measurements from TCCON and NDACC, as well as vertical profiles from AirCore, confirming the satellite data's accuracy and reliability.

Additionally, the application of the GEOS-Chem model to analyze PM_{2.5} emissions from the wildfires revealed their impact. The unprecedented emissions of 328 million tons of PM_{2.5}, particularly with California as a major contributor, represent a marked increase from previous years. This aspect of the research not only quantified the emissions but also shed light on the prolonged exposure of populations to harmful air quality with potential adverse public health implications.

Further research is necessary in several areas, particularly in integrating satellite data within modeling frameworks. This exploration could reveal if using satellite data to adjust fire

inventories improves the GEOS-Chem simulations, potentially aligning them more closely with station retrievals and improving their accuracy and reliability. Furthermore, there is an opportunity to integrate advanced satellite retrieval methods as inputs into top-down inventories. This method would utilize sophisticated satellite data to enhance the accuracy of modeling and analytical processes. The potential benefits of leveraging data from multiple satellites for improved model accuracy and more precise fire emission assessments are also worth investigating. Such an approach, especially with enhanced vertical estimations, may offer a pathway to more accurate emissions estimates.

This study highlights the need to integrate advanced tools and datasets for a comprehensive understanding of wildfires, which is crucial for adapting to climate change.

Appendices

Appendix A

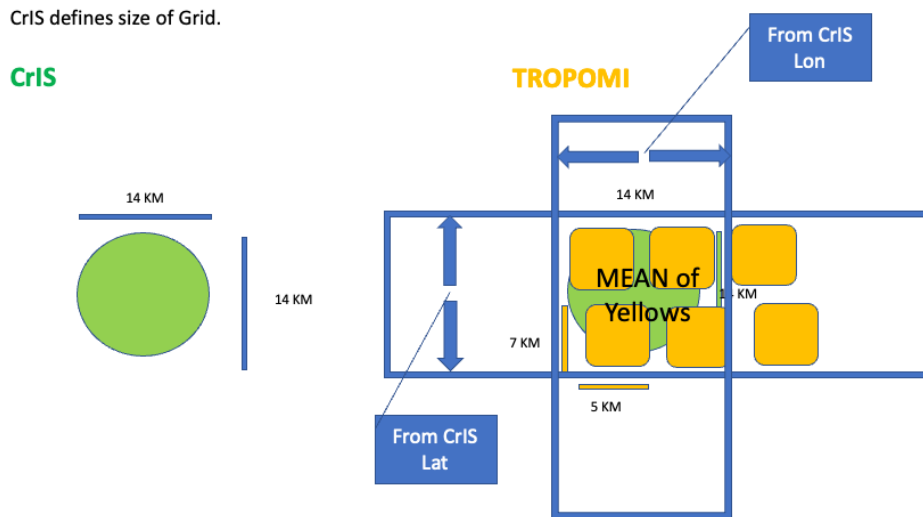


Figure A 1: Regridding approach used to obtain TROPOMI measurements with the resolution equivalent to CrIs. To homogenize TROPOMI, to CrIS resolution, we performed a weighted average of the pixels of TROPOMI that fall inside a CrIS Pixel using a square filter.

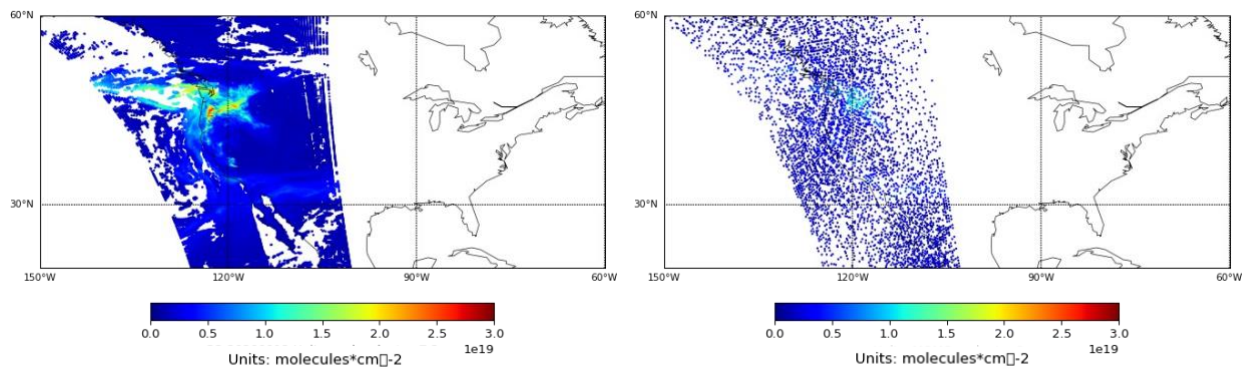
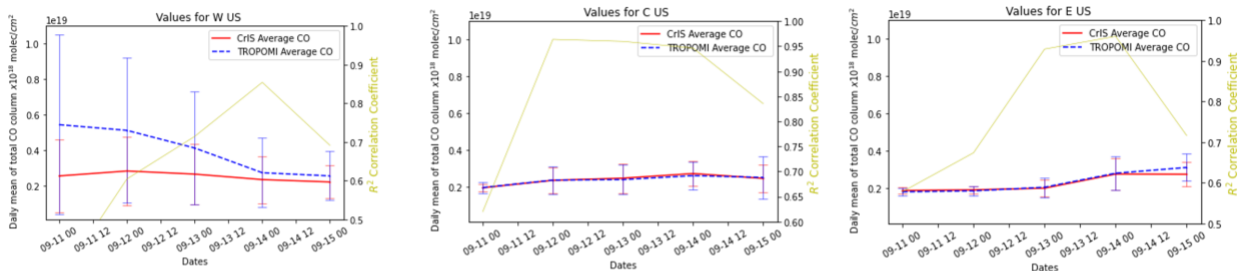


Figure A 2: Example of TROPOMI (left) and CrIS (right) and retrievals for the same swath.

0.25 Resolution



0.7 Resolution

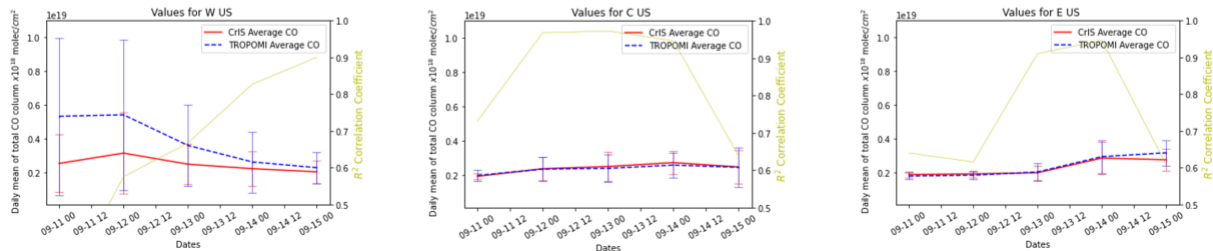


Figure A 3: Comparison of daily averages for the Western Central and Eastern regions of CrIS and TROPOMI using 0.25 degree resolution (top row) and 0.7 degree resolution (bottom row). The left column shows the West, the central column shows the central U.S. and the rightmost column shows the Eastern. The top row shows high-resolution measurements from CrIS at a resolution of 0.25, and the bottom row shows low resolution of CrIS.

Appendix B

Table B1: Percentage of fire PM_{2.5} emissions relative to the 2015-2020 total. The sum of the values in each state equals 100%.

	2015	2016	2017	2018	2019	2020
Arizona	7.3	18.9	19.8	12.0	14.6	27.3
California	9.7	7.6	14.0	14.1	3.8	50.8
Colorado	1.1	5.2	2.7	16.6	2.2	72.2
Idaho	29.9	20.0	22.9	11.3	6.3	9.6
Montana	18.7	9.7	57.3	6.0	3.5	4.8
Nevada	1.1	8.1	21.4	49.3	3.5	16.5
New Mexico	4.6	18.6	11.6	28.1	10.8	26.4
Oregon	14.3	7.3	22.2	13.6	5.4	37.2
Utah	3.0	9.9	24.3	41.3	5.7	15.8
Washington	52.6	3.7	18.4	10.7	4.6	10.0
Wyoming	1.9	25.6	2.9	23.1	2.5	43.9

Table B2: Statewide summary of the number of AQS stations, days of available data, and the correlation coefficient when compared to the corresponding GEOS-Chem grid cell for All-Sources and No-Fire.

	Number of Stations	Product of number of stations times days	Mean r ² (No Fire)	Mean r ² (All Sources)
Arizona	7	7577	0.02	0.03
California	56	60359	0.02	0.21
Colorado	4	4303	0.00	0.19
Idaho	1	1096	0.01	0.65
Montana	13	13908	0.02	0.45
Nevada	7	7609	0.00	0.24
New Mexico	4	4327	0.01	0.05
North Dakota	7	7459	0.01	0.37
South Dakota	4	4373	0.02	0.31
Utah	5	5336	0.00	0.18
Washington	10	10539	0.04	0.63
Wyoming	6	6191	0.01	0.34

Table B3: Area-Days of exposure to levels above the 35 $\mu\text{g}/\text{m}^3$ standard (in $\text{km}^2 \times \text{days}$). This table displays the area-days of exposure that each state experienced during the six-year period. To estimate such number we use smoke-specific PM_{2.5} concentrations, and select the grid cells that exceeded the 35 $\mu\text{g}/\text{m}^3$ EPA Standard, on each day. Then we calculate the number of days that each grid-cell was above the EPA Standard for each year and multiply it times the area of each of the grid cells. We then organize it by state.

	2015	2016	2017	2018	2019	2020
california	9.83E+05	7.7E+05	1.1E+06	1.6E+06	1.5E+05	5.4E+06
oregon	7.3E+05	1.3E+05	1.4E+06	9.8E+05	1.8E+05	2.0E+06
washington	1.1E+06	3.8E+04	1.5E+06	1.5E+06	6.6E+04	1.3E+06
idaho	8.8E+05	5.0E+05	1.1E+06	3.9E+05	1.5E+05	8.5E+05
montana	2.2E+06	2.2E+05	1.6E+06	1.1E+06	5.9E+04	5.9E+05
wyoming	1.2E+05	1.1E+05	5.8E+04	1.5E+05	1.3E+04	1.4E+05
nevada	6.0E+04	3.0E+04	1.1E+05	3.6E+05	7.0E+04	8.7E+05
utah	1.7E+04	2.7E+04	1.3E+05	2.1E+05	1.3E+04	2.0E+05
colorado	2.4E+04	2.8E+04	7.0E+04	2.3E+05	1.6E+04	8.9E+05
new mexico	0.0E+00	3.3E+04	2.4E+03	2.8E+04	4.0E+03	4.1E+04
arizona	8.0E+03	4.4E+04	5.8E+04	2.4E+04	5.0E+04	1.2E+05

Table B4: State-wide summary of the number of IMPROVE stations, days of available data, and the correlation coefficient when compared to the corresponding GEOS-Chem grid cell for All-Sources and No-Fire.

	Number of stations	Product of number of stations times days	Mean r^2 (No Fire)	Mean r^2 (All Sources)
Arizona	11	3838	0.02	0.08
California	18	6048	0.01	0.37
Colorado	8	2815	0.01	0.14
Idaho	2	668	0.01	0.39
Kansas	1	360	0.01	0.02
Montana	7	2395	0.02	0.42
Nebraska	1	352	0.02	0.09
Nevada	2	714	0.00	0.24
New Mexico	6	2003	0.01	0.10
North Dakota	2	709	0.01	0.39
Oregon	6	2067	0.01	0.48
South Dakota	2	725	0.02	0.27
Texas	1	341	0.01	0.03

Utah	4	1405	0.01	0.06
Washington	8	2781	0.01	0.57
Wyoming	4	1367	0.02	0.35

Table B5: Summary of State Populations in Millions and Land Areas in Square Kilometres.

	Population	Area
Arizona	6.7	2.90E+05
California	39	4.00E+05
Colorado	5.4	2.70E+05
Idaho	1.6	2.10E+05
Kansas	2.9	2.10E+05
Montana	1	3.80E+05
Nebraska	1.9	2.00E+05
Nevada	2.8	2.80E+05
New Mexico	2.1	3.10E+05
North Dakota	0.74	1.80E+05
Oregon	4	2.50E+05
South Dakota	0.85	1.96E+05
Texas	27	6.80E+05
Utah	2.9	2.10E+05
Washington	7.1	1.70E+05
Wyoming	0.58	2.50E+05

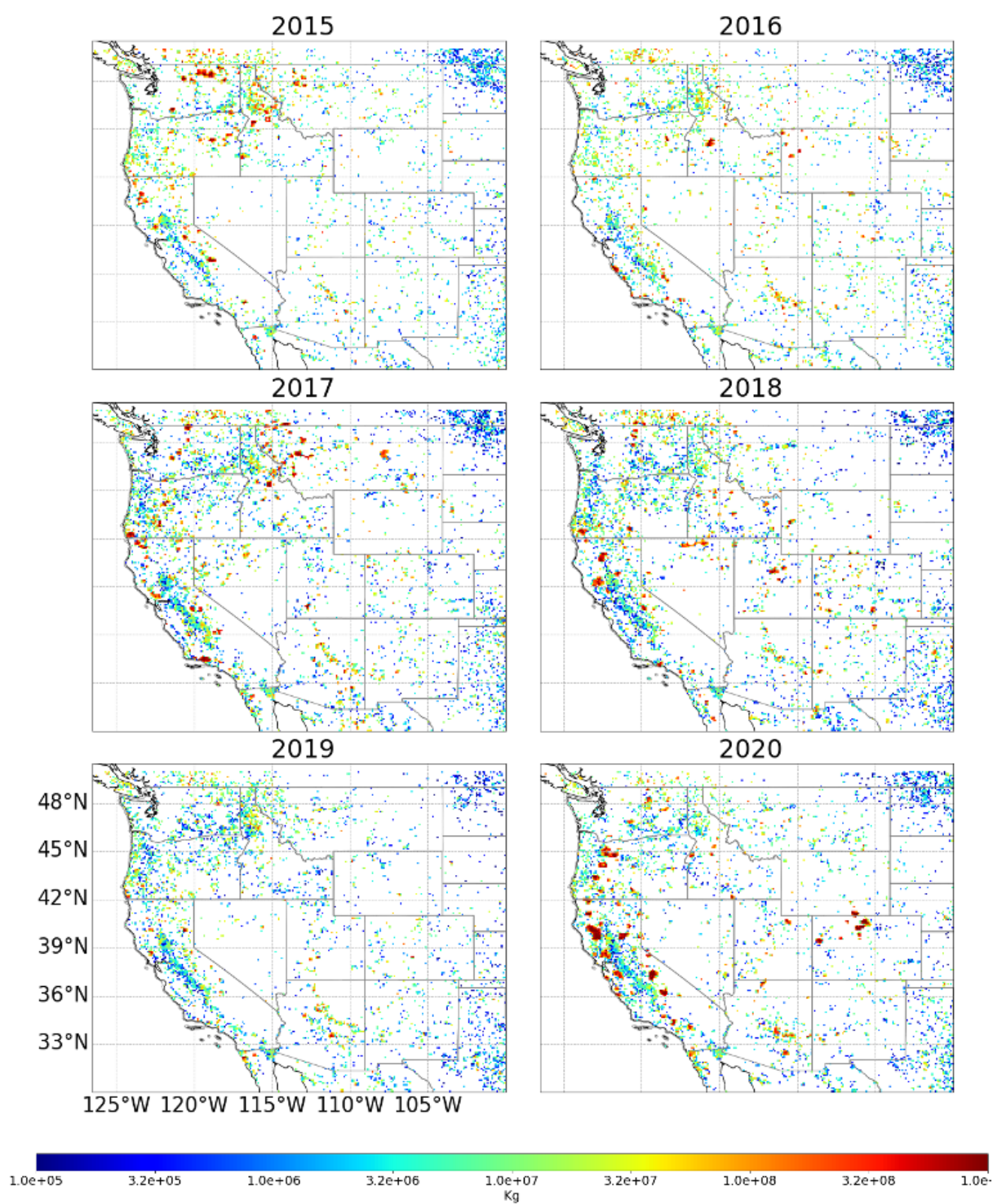


Figure B 1: Map of annual total GFAS emissions for 2015-2020 (in kg).



Figure B 2: We create daily time-series data for modeled PM_{2.5} by averaging values from the AQS monitoring stations within each GEOS-Chem cell. This process results in daily averages for the entire Western U.S. which are then averaged to obtain a daily average for the entire region. Additionally, to ensure data consistency, we include measurements from stations that provided data on at least 50% of days in each of the six years of the study period.

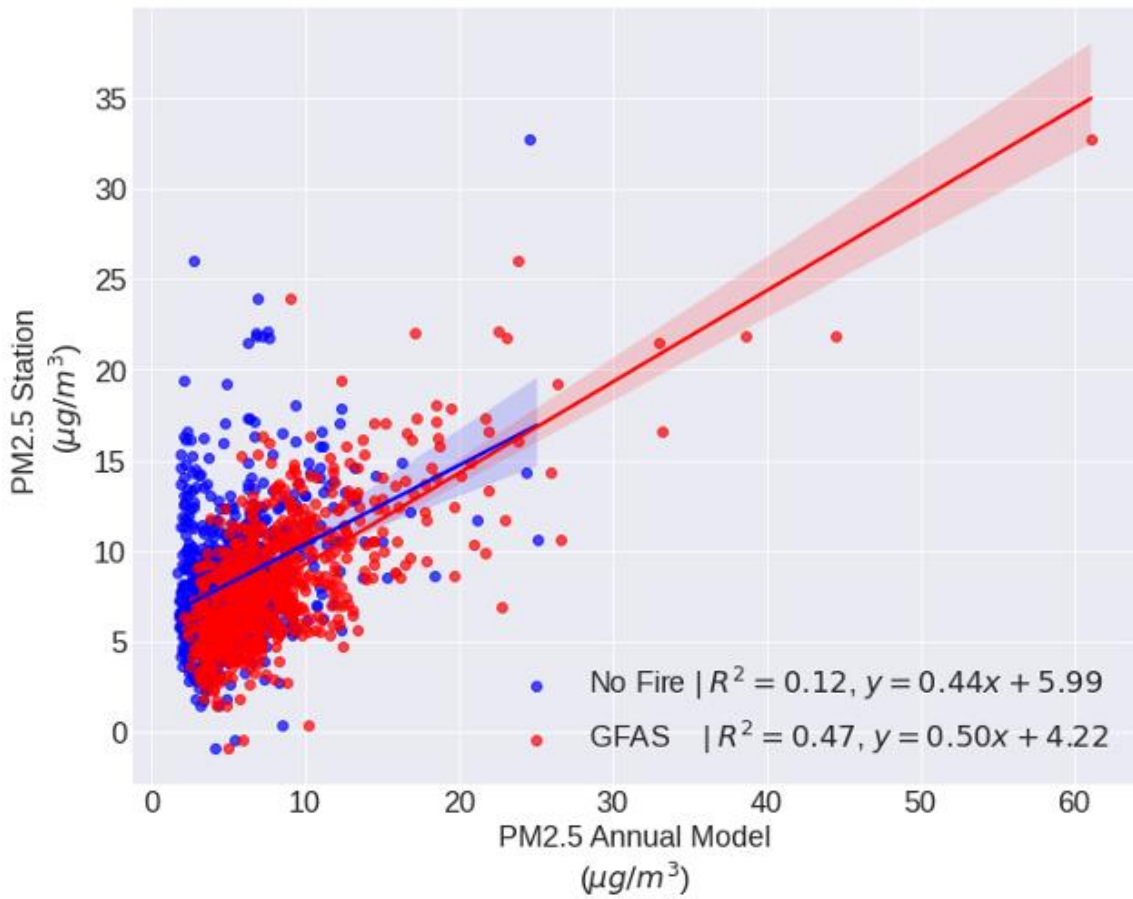


Figure B 3: We calculate the correlation between modeled PM2.5 and AQS station-based PM2.5 using average annual measurements for each year in the six-year period. This computation is based on matching days at each station and includes averaging data from multiple stations within the same GEOS-Chem grid cell. Each station location has six corresponding annual averages, encompassing measurements from both the monitor and GEOS-Chem. This analysis includes all stations across the Western U.S.



Figure B 4: We create time-series data for modeled PM_{2.5} by averaging values from the IMPROVE monitoring stations within each GEOS-Chem cell. IMPROVE data is available every three days, hence we obtain daily model estimates every three days which are then averaged to obtain a single daily average for the entire region. To ensure data consistency, we include measurements from stations that provided data for at least 50% of the three-day measurements in each of the six years of the study period.

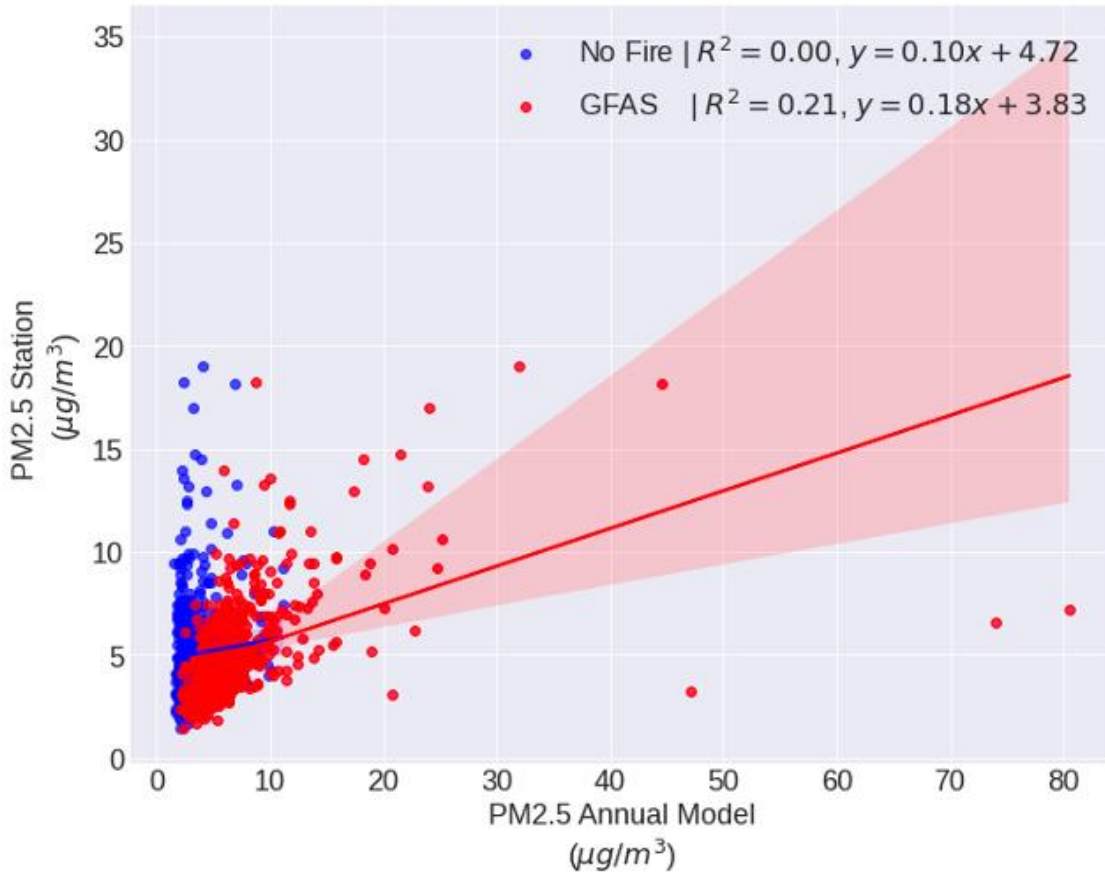


Figure B 5: We calculate the correlation between modeled PM2.5 and IMPROVE station-based PM2.5 using average annual measurements for each year in the six-year period. This computation is based on matching days at each station and includes averaging data from multiple stations within the same GEOS-Chem grid cell. Each station location has six corresponding annual averages, encompassing measurements from both the monitor and GEOS-Chem. This analysis includes all stations across the Western U.S.

References

- Adams, Cristen, Chris A. McLinden, Mark W. Shephard, Nolan Dickson, Enrico Dammers, Jack Chen, Paul Makar, et al. 2019. "Satellite-Derived Emissions of Carbon Monoxide, Ammonia, and Nitrogen Dioxide from the 2016 Horse River Wildfire in the Fort McMurray Area." *Atmospheric Chemistry and Physics* 19 (4): 2577–99. <https://doi.org/10.5194/acp-19-2577-2019>.
- Adetona O, Reinhardt T, Domitrovich J, Broyles G, Adetona AM, Kleinman MT, Kleinman RD, Roger DO, Naher LP (2016) Review of the health effects of wildland fire smoke on wildland firefighters and the public. *Inhalation Toxicology* 28, 95–139. doi:10.3109/08958378.2016.1145771
- Aguilera, Rosana, Nana Luo, Rupa Basu, Jun Wu, Rachel Clemesha, Alexander Gershunov, and Tarik Benmarhnia. 2023. "A Novel Ensemble-Based Statistical Approach to Estimate Daily Wildfire-Specific PM_{2.5} in California (2006–2020)." *Environment International* 171 (January): 107719. <https://doi.org/10.1016/j.envint.2022.107719>.
- Aguilera, Rosana, Thomas Corringham, Alexander Gershunov, and Tarik Benmarhnia. 2021. "Wildfire Smoke Impacts Respiratory Health More than Fine Particles from Other Sources: Observational Evidence from Southern California." *Nature Communications* 12 (1): 1493. <https://doi.org/10.1038/s41467-021-21708-0>.
- Albery, Gregory F., Isabella Turilli, Maxwell B. Joseph, Janet Foley, Celine H. Frere, and Shweta Bansal. 2021. "From Flames to Inflammation: How Wildfires Affect Patterns of Wildlife Disease." *Fire Ecology* 17 (1): 23. <https://doi.org/10.1186/s42408-021-00113-4>.

Albores, I.S., R.R. Buchholz, I. Ortega, L.K. Emmons, J.W. Hannigan, F. Lacey, G. Pfister, W. Tang, and H.M. Worden. 2023. “Continental-Scale Atmospheric Impacts of the 2020 Western U.S. Wildfires.” *Atmospheric Environment* 294 (February): 119436.
<https://doi.org/10.1016/j.atmosenv.2022.119436>.

Albores, I.S., R.R. Buchholz, I. Ortega, L.K. Emmons, J.W. Hannigan, F. Lacey, G. Pfister, W. Tang, and H.M. Worden. 2023. “Continental-Scale Atmospheric Impacts of the 2020 Western U.S. Wildfires.” *Atmospheric Environment* 294 (February): 119436.
<https://doi.org/10.1016/j.atmosenv.2022.119436>.

Al-Hamdan, Mohammad Z., William L. Crosson, Sigrid A. Economou, Maurice G. Estes, Sue M. Estes, Sarah N. Hemmings, Shia T. Kent, et al. 2014. “Environmental Public Health Applications Using Remotely Sensed Data.” *Geocarto International* 29 (1): 85–98.
<https://doi.org/10.1080/10106049.2012.715209>.

Andreae, Meinrat O. 2019. “Emission of Trace Gases and Aerosols from Biomass Burning –An Updated Assessment.” Preprint. *Biosphere Interactions/Field Measurements/Troposphere/Chemistry (chemical composition and reactions)*.
<https://doi.org/10.5194/acp-2019-303>.

Bernstein, D.N., Hamilton, D.S., Krasnoff, R., Mahowald, N.M., Connelly, D.S., Tilmes, S., Hess, P.G., 2021. Short-term impacts of 2017 western North American wildfires on meteorology, the atmosphere’s energy budget, and premature mortality. *Environ. Res. Lett.* 16 (6), 064065.

- Black, Carolyn, Yohannes Tesfaigzi, Jed A. Bassein, and Lisa A. Miller. 2017. “Wildfire Smoke Exposure and Human Health: Significant Gaps in Research for a Growing Public Health Issue.” *Environmental Toxicology and Pharmacology* 55 (October): 186–95.
<https://doi.org/10.1016/j.etap.2017.08.022>.
- Bloom, H.J. 2001. “The Cross-Track Infrared Sounder (CrIS): A Sensor for Operational Meteorological Remote Sensing.” In *IGARSS 2001. Scanning the Present and Resolving the Future. Proceedings. IEEE 2001 International Geoscience and Remote Sensing Symposium (Cat. No.01CH37217)*, 3:1341–43. Sydney, NSW, Australia: IEEE.
<https://doi.org/10.1109/IGARSS.2001.976838>.
- Borsdorff, T., J. Aan de Brugh, H. Hu, I. Aben, O. Hasekamp, and J. Landgraf. 2018. “Measuring Carbon Monoxide With TROPOMI: First Results and a Comparison With ECMWF-IFS Analysis Data.” *Geophysical Research Letters* 45 (6): 2826–32.
<https://doi.org/10.1002/2018GL077045>.
- Borsdorff, T., O. P. Hasekamp, A. Wassmann, and J. Landgraf. 2014. “Insights into Tikhonov Regularization: Application to Trace Gas Column Retrieval and the Efficient Calculation of Total Column Averaging Kernels.” *Atmospheric Measurement Techniques* 7 (2): 523–35. <https://doi.org/10.5194/amt-7-523-2014>.
- Borsdorff, Tobias, Agustín García Reynoso, Gilberto Maldonado, Bertha Mar-Morales, Wolfgang Stremme, Michel Grutter, and Jochen Landgraf. 2020. “Monitoring CO Emissions of the Metropolis Mexico City Using TROPOMI CO Observations.” *Atmospheric Chemistry and Physics* 20 (24): 15761–74. <https://doi.org/10.5194/acp-20-15761-2020>.

- Bowman, K.W., C.D. Rodgers, S.S. Kulawik, J. Worden, E. Sarkissian, G. Osterman, T. Steck, et al. 2006. "Tropospheric Emission Spectrometer: Retrieval Method and Error Analysis." *IEEE Transactions on Geoscience and Remote Sensing* 44 (5): 1297–1307. <https://doi.org/10.1109/TGRS.2006.871234>.
- Bowman, Kevin W., Tilman Steck, Helen M. Worden, John Worden, Shepard Clough, and Clive Rodgers. 2002. "Capturing Time and Vertical Variability of Tropospheric Ozone: A Study Using TES Nadir Retrievals: CAPTURING OZONE TIME AND VERTICAL VARIABILITY." *Journal of Geophysical Research: Atmospheres* 107 (D23): ACH 21-1-ACH 21-11. <https://doi.org/10.1029/2002JD002150>.
- Buchholz, Rebecca R., Merritt N. Deeter, Helen M. Worden, John Gille, David P. Edwards, James W. Hannigan, Nicholas B. Jones, et al. 2017. "Validation of MOPITT Carbon Monoxide Using Ground-Based Fourier Transform Infrared Spectrometer Data from NDACC." *Atmospheric Measurement Techniques* 10 (5): 1927–56. <https://doi.org/10.5194/amt-10-1927-2017>.
- Burke, Marshall, Sam Heft-Neal, Jessica Li, Anne Driscoll, Patrick Baylis, Matthieu Stigler, Joakim A. Weill, et al. 2022. "Exposures and Behavioural Responses to Wildfire Smoke." *Nature Human Behaviour* 6 (10): 1351–61. <https://doi.org/10.1038/s41562-022-01396-6>.
- Burrows, J.P, H Bovensmann, G Bergametti, J.M Flaud, J Orphal, S Noël, P.S Monks, et al. 2004. "The Geostationary Tropospheric Pollution Explorer (GeoTROPE) Mission: Objectives, Requirements and Mission Concept." *Advances in Space Research* 34 (4): 682–87. <https://doi.org/10.1016/j.asr.2003.08.067>.

C. P. Rinsland, A. Goldman, J. W. Hannigan, S. W. Wood, L. S. Chiou, and E. Mahieu. 2007.

“Long-Term Trends of Tropospheric Carbon Monoxide and Hydrogen Cyanide from Analysis of High Resolution Infrared Solar Spectra.” *J. Quant. Spectrosc. Radiat. Transfer* 104: 40–51.

Cal Fire. 2023. “2020 Incident Archive.” <https://www.fire.ca.gov/incidents/2020>.

Carter T S et al 2020 How emissions uncertainty influences the distribution and radiative impacts of smoke from fires in North America *Atmos. Chem. Phys.* 20 2073–97

Center For International Earth Science Information Network-CIESIN-Columbia University.

2018. “Gridded Population of the World, Version 4 (GPWv4): Population Count, Revision 11.” Palisades, NY: NASA Socioeconomic Data and Applications Center (SEDAC). <https://doi.org/10.7927/H4JW8BX5>.

Chance, Kelly V., and Robert J. D. Spurr. 1997. “Ring Effect Studies: Rayleigh Scattering, Including Molecular Parameters for Rotational Raman Scattering, and the Fraunhofer Spectrum.” *Applied Optics* 36 (21): 5224. <https://doi.org/10.1364/AO.36.005224>.

Childs, Marissa L., Jessica Li, Jeffrey Wen, Sam Heft-Neal, Anne Driscoll, Sherrie Wang, Carlos F. Gould, Minghao Qiu, Jennifer Burney, and Marshall Burke. 2022. “Daily Local-Level Estimates of Ambient Wildfire Smoke PM 2.5 for the Contiguous US.” *Environmental Science & Technology* 56 (19): 13607–21. <https://doi.org/10.1021/acs.est.2c02934>.

Cleland, Stephanie E., J. Jason West, Yiqin Jia, Stephen Reid, Sean Raffuse, Susan O’Neill, and Marc L. Serre. 2020. “Estimating Wildfire Smoke Concentrations during the October 2017 California Fires through BME Space/Time Data Fusion of Observed, Modeled, and

- Satellite-Derived PM 2.5.” *Environmental Science & Technology* 54 (21): 13439–47.
<https://doi.org/10.1021/acs.est.0c03761>.
- Clerbaux, C., A. Boynard, L. Clarisse, M. George, J. Hadji-Lazaro, H. Herbin, D. Hurtmans, et al. 2009. “Monitoring of Atmospheric Composition Using the Thermal Infrared IASI/MetOp Sounder.” *Atmospheric Chemistry and Physics* 9 (16): 6041–54.
<https://doi.org/10.5194/acp-9-6041-2009>.
- Coop, Jonathan D, Sean A Parks, Camille S Stevens-Rumann, Shelley D Crausbay, Philip E Higuera, Matthew D Hurteau, Alan Tepley, et al. 2020. “Wildfire-Driven Forest Conversion in Western North American Landscapes.” *BioScience* 70 (8): 659–73.
<https://doi.org/10.1093/biosci/biaa061>.
- Csiszar, Ivan, Walter Wolf, Louis Giglio, Wilfrid Schroeder, Zhaohui Cheng, and NOAA JPSS Program Office. 2016. “JPSS VIIRS Active Fires (AF) EDR from NDE.” NOAA National Centers for Environmental Information. <https://doi.org/10.7289/V5GH9G0T>.
- Cuesta, J., M. Eremenko, X. Liu, G. Dufour, Z. Cai, M. Höpfner, T. Von Clarmann, et al. 2013. “Satellite Observation of Lowermost Tropospheric Ozone by Multispectral Synergism of IASI Thermal Infrared and GOME-2 Ultraviolet Measurements over Europe.” *Atmospheric Chemistry and Physics* 13 (19): 9675–93. <https://doi.org/10.5194/acp-13-9675-2013>.
- Dammers, Enrico, Mark W. Shephard, Mathias Palm, Karen Cady-Pereira, Shannon Capps, Erik Lutsch, Kim Strong, et al. 2017. “Validation of the CrIS Fast Physical

- NH<Sub>3</Sub> Retrieval with Ground-Based FTIR.” *Atmospheric Measurement Techniques* 10 (7): 2645–67. <https://doi.org/10.5194/amt-10-2645-2017>.
- Deeter, M. N., S. Martínez-Alonso, D. P. Edwards, L. K. Emmons, J. C. Gille, H. M. Worden, C. Sweeney, J. V. Pittman, B. C. Daube, and S. C. Wofsy. 2014. “The MOPITT Version 6 Product: Algorithm Enhancements and Validation.” *Atmospheric Measurement Techniques* 7 (11): 3623–32. <https://doi.org/10.5194/amt-7-3623-2014>.
- Delfino, R J, S Brummel, J Wu, H Stern, B Ostro, M Lipsett, A Winer, et al. 2009. “The Relationship of Respiratory and Cardiovascular Hospital Admissions to the Southern California Wildfires of 2003.” *Occupational and Environmental Medicine* 66 (3): 189–97. <https://doi.org/10.1136/oem.2008.041376>.
- Deutscher, N. M., D. W. T. Griffith, G. W. Bryant, P. O. Wennberg, G. C. Toon, R. A. Washenfelder, G. Keppel-Aleks, et al. 2010. “Total Column CO<Sub>2</Sub> Measurements at Darwin, Australia – Site Description and Calibration against in Situ Aircraft Profiles.” *Atmospheric Measurement Techniques* 3 (4): 947–58. <https://doi.org/10.5194/amt-3-947-2010>.
- Di Giuseppe, Francesca, Samuel Rémy, Florian Pappenberger, and Fredrik Wetterhall. 2018. “Using the Fire Weather Index (FWI) to Improve the Estimation of Fire Emissions from Fire Radiative Power (FRP) Observations.” *Atmospheric Chemistry and Physics* 18 (8): 5359–70. <https://doi.org/10.5194/acp-18-5359-2018>.
- Di, Qian, Heresh Amini, Liuhua Shi, Itai Kloog, Rachel Silvern, James Kelly, M. Benjamin Sabath, et al. 2019. “An Ensemble-Based Model of PM_{2.5} Concentration across the

- Contiguous United States with High Spatiotemporal Resolution.” *Environment International* 130 (September): 104909. <https://doi.org/10.1016/j.envint.2019.104909>.
- Dittrich R and McCallum S 2020 How to measure the economic health cost of wildfires—a systematic review of the literature for northern America *Int. J. Wildland Fire* 29 961–73
- Drummond, James R., Jiansheng Zou, Florian Nichitiu, Jayanta Kar, Robert Deschambaut, and John Hackett. 2010. “A Review of 9-Year Performance and Operation of the MOPITT Instrument.” *Advances in Space Research* 45 (6): 760–74. <https://doi.org/10.1016/j.asr.2009.11.019>.
- Environmental Protection Agency. 2016. “NAAQS Table.” Washington, United States. <https://www.epa.gov/criteria-air-pollutants/naaqs-table>.
- ESA. 2023. “TROPOMI Level 2 Carbon Monoxide Total Column.” <https://doi.org/10.5270/S5P-1hkp7rp>.
- Fu, Dejian, Kevin W. Bowman, Helen M. Worden, Vijay Natraj, John R. Worden, Shanshan Yu, Pepijn Veefkind, et al. 2016. “High-Resolution Tropospheric Carbon Monoxide Profiles Retrieved from CrIS and TROPOMI.” *Atmospheric Measurement Techniques* 9 (6): 2567–79. <https://doi.org/10.5194/amt-9-2567-2016>.
- Fu, Dejian, Susan S. Kulawik, Kazuyuki Miyazaki, Kevin W. Bowman, John R. Worden, Annmarie Eldering, Nathaniel J. Livesey, et al. 2018. “Retrievals of Tropospheric Ozone Profiles from the Synergism of AIRS and OMI: Methodology and Validation.” *Atmospheric Measurement Techniques* 11 (10): 5587–5605. <https://doi.org/10.5194/amt-11-5587-2018>.

- Gantt, Brett, Kelsey McDonald, Barron Henderson, and Elizabeth Mannshardt. 2020. “Incorporation of Remote PM_{2.5} Concentrations into the Downscaler Model for Spatially Fused Air Quality Surfaces.” *Atmosphere* 11 (1): 103. <https://doi.org/10.3390/atmos11010103>.
- George, M., C. Clerbaux, I. Bouarar, P.-F. Coheur, M. N. Deeter, D. P. Edwards, G. Francis, et al. 2015. “An Examination of the Long-Term CO Records from MOPITT and IASI: Comparison of Retrieval Methodology.” *Atmospheric Measurement Techniques* 8 (10): 4313–28. <https://doi.org/10.5194/amt-8-4313-2015>.
- Halofsky, Jessica E., David L. Peterson, and Brian J. Harvey. 2020. “Changing Wildfire, Changing Forests: The Effects of Climate Change on Fire Regimes and Vegetation in the Pacific Northwest, USA.” *Fire Ecology* 16 (1): 4. <https://doi.org/10.1186/s42408-019-0062-8>.
- Hamilton D S, Hantson S, Scott C E, Kaplan J O, Pringle K J, Nieradzik L P, Rap A, Folberth G A, Spracklen D V and Carslaw K S 2018 Reassessment of pre-industrial fire emissions strongly affects anthropogenic aerosol forcing *Nat. Commun.* 9 3182
- Hanninen OO, Salonen RO, Koistinen K, Lanki T, Barregard L, Jantunen M (2009) Population exposure to fine particles and estimated excess mortality in Finland from an eastern European wildfire episode. *Journal of Exposure Science & Environmental Epidemiology* 19, 414–422. doi:10.1038/JES.2008.31
- Hase, F., J.W. Hannigan, M.T. Coffey, A. Goldman, M. Höpfner, N.B. Jones, C.P. Rinsland, and S.W. Wood. 2004. “Intercomparison of Retrieval Codes Used for the Analysis of High-

- Resolution, Ground-Based FTIR Measurements.” *Journal of Quantitative Spectroscopy and Radiative Transfer* 87 (1): 25–52. <https://doi.org/10.1016/j.jqsrt.2003.12.008>.
- Hedelius, Jacob K., Junjie Liu, Tomohiro Oda, Shamil Maksyutov, Coleen M. Roehl, Laura T. Iraci, James R. Podolske, et al. 2018. “Southern California Megacity CO₂, CH₄, and CO Flux Estimates Using Ground- and Space-Based Remote Sensing and a Lagrangian Model.” *Atmospheric Chemistry and Physics* 18 (22): 16271–91. <https://doi.org/10.5194/acp-18-16271-2018>.
- Higuera, Philip E., and John T. Abatzoglou. 2021. “Record-setting Climate Enabled the Extraordinary 2020 Fire Season in the Western United States.” *Global Change Biology* 27 (1): 1–2. <https://doi.org/10.1111/gcb.15388>.
- Hochstaffl, Philipp, Franz Schreier, Günter Lichtenberg, and Sebastian Gimeno García. 2018. “Addendum: Hochstaffl, P. et al. Validation of Carbon Monoxide Total Columns from SCIAMACHY with NDACC/TCCON Ground-Based Measurements. *Remote Sens.* 2018, 10, 223.” *Remote Sensing* 10 (3): 469. <https://doi.org/10.3390/rs10030469>.
- Hoek, Gerard, Rob Beelen, Kees De Hoogh, Danielle Vienneau, John Gulliver, Paul Fischer, and David Briggs. 2008. “A Review of Land-Use Regression Models to Assess Spatial Variation of Outdoor Air Pollution.” *Atmospheric Environment* 42 (33): 7561–78. <https://doi.org/10.1016/j.atmosenv.2008.05.057>.

Iglesias, Virginia, Jennifer K. Balch, and William R. Travis. 2022. “U.S. Fires Became Larger, More Frequent, and More Widespread in the 2000s.” *Science Advances* 8 (11): eabc0020. <https://doi.org/10.1126/sciadv.abc0020>.

Intergovernmental Panel On Climate Change. 2023. *Climate Change 2021 – The Physical Science Basis: Working Group I Contribution to the Sixth Assessment Report of the Intergovernmental Panel on Climate Change*. 1st ed. Cambridge University Press. <https://doi.org/10.1017/9781009157896>.

Jacobsen, Anna L., and R. Brandon Pratt. 2018. “Extensive Drought-associated Plant Mortality as an Agent of Type-conversion in Chaparral Shrublands.” *New Phytologist* 219 (2): 498–504. <https://doi.org/10.1111/nph.15186>.

J. L. Laughner, G. C. Toon, D. Wunch, S. Roche, J. Mendonca, M. Kiel, C. M. Roehl, C. Petri, and P. O. Wennberg. 2023. “The Total Carbon Column Observing Network’s GGG2020.” <http://www.tccon.caltech.edu/>.

Jerrett, Michael, Amir S. Jina, and Miriam E. Marlier. 2022. “Up in Smoke: California’s Greenhouse Gas Reductions Could Be Wiped out by 2020 Wildfires.” *Environmental Pollution* 310 (October): 119888. <https://doi.org/10.1016/j.envpol.2022.119888>.

Johnson, Matthew S., Alexei Rozanov, Mark Weber, Nora Mettig, John Sullivan, Michael J. Newchurch, Shi Kuang, et al. 2023. “TOLNet Validation of Satellite Ozone Profiles in the Troposphere: Impact of Retrieval Wavelengths.” Preprint. *Gases/Remote*

- Johnston F, Hanigan I, Henderson S, Morgan G, Bowman D (2011) Extreme air pollution from bushfires and dust storms and their association with mortality in Sydney, Australia 1994–2007. *Environmental Research* 111, 811–816. doi:10.1016/J.ENVRES.2011.05.007
- K.E. Knowland, C.A. Keller, and R. Lucchesi. 2020. “File Specification for GEOS-CF Products.” GMAO Office. http://gmao.gsfc.nasa.gov/pubs/office_notes.
- Kaiser, J. W., A. Heil, M. O. Andreae, A. Benedetti, N. Chubarova, L. Jones, J.-J. Morcrette, et al. 2012. “Biomass Burning Emissions Estimated with a Global Fire Assimilation System Based on Observed Fire Radiative Power.” *Biogeosciences* 9 (1): 527–54. <https://doi.org/10.5194/bg-9-527-2012>.
- Karion, Anna, Colm Sweeney, Pieter Tans, and Timothy Newberger. 2010. “AirCore: An Innovative Atmospheric Sampling System.” *Journal of Atmospheric and Oceanic Technology* 27 (11): 1839–53. <https://doi.org/10.1175/2010JTECHA1448.1>.
- Kaufman, Y. J., C. Ichoku, L. Giglio, S. Korontzi, D. A. Chu, W. M. Hao, R.-R. Li, and C. O. Justice. 2003. “Fire and Smoke Observed from the Earth Observing System MODIS Instrument--Products, Validation, and Operational Use.” *International Journal of Remote Sensing* 24 (8): 1765–81. <https://doi.org/10.1080/01431160210144741>.
- Keeley, Jon E., and Alexandra D. Syphard. 2021. “Large California Wildfires: 2020 Fires in Historical Context.” *Fire Ecology* 17 (1): 22. <https://doi.org/10.1186/s42408-021-00110-7>.
- Kiel, Matthäus, Frank Hase, Thomas Blumenstock, and Oliver Kirner. 2016. “Comparison of XCO Abundances from the Total Carbon Column Observing Network and the Network

for the Detection of Atmospheric Composition Change Measured in Karlsruhe.”

Atmospheric Measurement Techniques 9 (5): 2223–39. <https://doi.org/10.5194/amt-9-2223-2016>.

Kim, Yong Ho, Sarah H. Warren, Q. Todd Krantz, Charly King, Richard Jaskot, William T.

Preston, Barbara J. George, et al. 2018. “Mutagenicity and Lung Toxicity of Smoldering vs. Flaming Emissions from Various Biomass Fuels: Implications for Health Effects from Wildland Fires.” *Environmental Health Perspectives* 126 (1): 017011.

<https://doi.org/10.1289/EHP2200>.

Kochi I, Champ PA, Loomis JB, Donovan GH (2016) Valuing morbidity effects of wildfire

smoke exposure from the 2007 southern California wildfires. *Journal of Forest*

Economics 25, 29–54. doi:10.1016/J.JFE. 2016.07.002

Krol, M., S. Houweling, B. Bregman, M. Van Den Broek, A. Segers, P. Van Velthoven, W. Peters,

F. Dentener, and P. Bergamaschi. 2005. “The Two-Way Nested Global Chemistry-

Transport Zoom Model TM5: Algorithm and Applications.” *Atmospheric Chemistry and*

Physics 5 (2): 417–32. <https://doi.org/10.5194/acp-5-417-2005>.

Kumar, Sujay, Augusto Getirana, Renata Libonati, Christopher Hain, Sarith Mahanama, and

Niels Andela. 2022. “Changes in Land Use Enhance the Sensitivity of Tropical

Ecosystems to Fire-Climate Extremes.” *Scientific Reports* 12 (1): 964.

<https://doi.org/10.1038/s41598-022-05130-0>.

Landgraf, J., and O. P. Hasekamp. 2007. “Retrieval of Tropospheric Ozone: The Synergistic Use

of Thermal Infrared Emission and Ultraviolet Reflectivity Measurements from Space.”

Journal of Geophysical Research 112 (D8): D08310.

<https://doi.org/10.1029/2006JD008097>.

Landgraf, Jochen, Joost Aan De Brugh, Remco Scheepmaker, Tobias Borsdorff, Haili Hu, Sander Houweling, Andre Butz, Ilse Aben, and Otto Hasekamp. 2016. “Carbon Monoxide Total Column Retrievals from TROPOMI Shortwaveinfrared Measurements.” *Atmospheric Measurement Techniques* 9 (10): 4955–75. <https://doi.org/10.5194/amt-9-4955-2016>.

Langerock, B., M. De Mazière, F. Hendrick, C. Vigouroux, F. Desmet, B. Dils, and S. Niemeijer. 2015. “Description of Algorithms for Co-Locating and Comparing Gridded Model Data with Remote-Sensing Observations.” *Geoscientific Model Development* 8 (3): 911–21. <https://doi.org/10.5194/gmd-8-911-2015>.

Langmann, Bärbel, Bryan Duncan, Christiane Textor, Jörg Trentmann, and Guido R. van der Werf. 2009. “Vegetation Fire Emissions and Their Impact on Air Pollution and Climate.” *Atmospheric Environment* (1994) 43 (1): 107–16. <https://doi.org/10.1016/j.atmosenv.2008.09.047>.

Lassman, William, Bonne Ford, Ryan W. Gan, Gabriele Pfister, Sheryl Magzamen, Emily V. Fischer, and Jeffrey R. Pierce. 2017. “Spatial and Temporal Estimates of Population Exposure to Wildfire Smoke during the Washington State 2012 Wildfire Season Using Blended Model, Satellite, and in Situ Data: Multimethod Estimates of Smoke Exposure.” *GeoHealth* 1 (3): 106–21. <https://doi.org/10.1002/2017GH000049>.

Latsch, Miriam, Andreas Richter, Henk Eskes, Maarten Sneep, Ping Wang, Pepijn Veeffkind, Ronny Lutz, et al. 2022. “Intercomparison of Sentinel-5P TROPOMI Cloud Products for

- Tropospheric Trace Gas Retrievals.” *Atmospheric Measurement Techniques* 15 (21): 6257–83. <https://doi.org/10.5194/amt-15-6257-2022>.
- Laughner, Joshua L., Jessica L. Neu, David Schimel, Paul O. Wennberg, Kelley Barsanti, Kevin W. Bowman, Abhishek Chatterjee, et al. 2021. “Societal Shifts Due to COVID-19 Reveal Large-Scale Complexities and Feedbacks between Atmospheric Chemistry and Climate Change.” *Proceedings of the National Academy of Sciences - PNAS* 118 (46): 1. <https://doi.org/10.1073/pnas.2109481118>.
- Lelieveld, Jos, Sergey Gromov, Andrea Pozzer, and Domenico Taraborrelli. 2016. “Global Tropospheric Hydroxyl Distribution, Budget and Reactivity.” *Atmospheric Chemistry and Physics* 16 (19): 12477–93. <https://doi.org/10.5194/acp-16-12477-2016>.
- Levine, J.S. 2014. “Biomass Burning: The Cycling of Gases and Particulates from the Biosphere to the Atmosphere.” In *Treatise on Geochemistry*, 139–50. Elsevier. <https://doi.org/10.1016/B978-0-08-095975-7.00405-8>.
- Lim, Chul-Hee, Jieun Ryu, Yuyoung Choi, Seong Woo Jeon, and Woo-Kyun Lee. 2020. “Understanding Global PM_{2.5} Concentrations and Their Drivers in Recent Decades (1998–2016).” *Environment International* 144 (November): 106011. <https://doi.org/10.1016/j.envint.2020.106011>.
- Liu, Jia C., Gavin Pereira, Sarah A. Uhl, Mercedes A. Bravo, and Michelle L. Bell. 2015. “A Systematic Review of the Physical Health Impacts from Non-Occupational Exposure to Wildfire Smoke.” *Environmental Research* 136 (January): 120–32. <https://doi.org/10.1016/j.envres.2014.10.015>.

- Liu, Jia Coco, Ander Wilson, Loretta J. Mickley, Francesca Dominici, Keita Ebisu, Yun Wang, Melissa P. Sulprizio, et al. 2017. “Wildfire-Specific Fine Particulate Matter and Risk of Hospital Admissions in Urban and Rural Counties.” *Epidemiology (Cambridge, Mass.)* 28 (1): 77–85. <https://doi.org/10.1097/EDE.0000000000000556>.
- Liu, Jia Coco, Loretta J. Mickley, Melissa P. Sulprizio, Francesca Dominici, Xu Yue, Keita Ebisu, Georgiana Brooke Anderson, Rafi F. A. Khan, Mercedes A. Bravo, and Michelle L. Bell. 2016. “Particulate Air Pollution from Wildfires in the Western US under Climate Change.” *Climatic Change* 138 (3–4): 655–66. <https://doi.org/10.1007/s10584-016-1762-6>.
- Liu, Tianjia, Loretta J. Mickley, Miriam E. Marlier, Ruth S. DeFries, Md Firoz Khan, Mohd Talib Latif, and Alexandra Karambelas. 2020. “Diagnosing Spatial Biases and Uncertainties in Global Fire Emissions Inventories: Indonesia as Regional Case Study.” *Remote Sensing of Environment* 237 (February): 111557. <https://doi.org/10.1016/j.rse.2019.111557>.
- Lloyd, Christopher T., Alessandro Sorichetta, and Andrew J. Tatem. 2017. “High Resolution Global Gridded Data for Use in Population Studies.” *Scientific Data* 4 (1): 170001. <https://doi.org/10.1038/sdata.2017.1>.
- Luo, Ming, William Read, Susan Kulawik, John Worden, Nathaniel Livesey, Kevin Bowman, and Robert Herman. 2013. “Carbon Monoxide (CO) Vertical Profiles Derived from Joined TES and MLS Measurements: CO PROFILES DERIVED FROM TES AND MLS.” *Journal of Geophysical Research: Atmospheres* 118 (18): 10,601–10,613. <https://doi.org/10.1002/jgrd.50800>.

Makkaroon, P., D. Q. Tong, Y. Li, E. J. Hyer, P. Xian, S. Kondragunta, P. C. Campbell, et al.

2023. “Development and Evaluation of a North America Ensemble Wildfire Air Quality Forecast: Initial Application to the 2020 Western United States ‘Gigafire.’” *Journal of Geophysical Research: Atmospheres* 128 (22): e2022JD037298.

<https://doi.org/10.1029/2022JD037298>.

Malina, Edward, Kevin W. Bowman, Valentin Kantchev, Le Kuai, Thomas P. Kurosu, Kazuyuki

Miyazaki, Vijay Natraj, Gregory B. Osterman, and Matthew D. Thill. 2022. “Joint Spectral Retrievals of Ozone with Suomi NPP CrIS Augmented by S5P/TROPOMI.”

Preprint. *Gases/Remote Sensing/Validation and Intercomparisons*.

<https://doi.org/10.5194/egusphere-2022-774>.

Marlier, Miriam E, Mu Xiao, Ruth Engel, Ben Livneh, John T Abatzoglou, and Dennis P

Lettenmaier. 2017. “The 2015 Drought in Washington State: A Harbinger of Things to Come?” *Environmental Research Letters* 12 (11): 114008. <https://doi.org/10.1088/1748-9326/aa8fde>.

Marlier, Miriam E, Katherine I Brenner, Jia Coco Liu, Loretta J Mickley, Sierra Raby, Eric

James, Ravan Ahmadov, and Heather Riden. 2022. “Exposure of Agricultural Workers in California to Wildfire Smoke under Past and Future Climate Conditions.” *Environmental Research Letters* 17 (9): 094045. <https://doi.org/10.1088/1748-9326/ac8c58>.

Martínez-Alonso, Sara, Merritt Deeter, Helen Worden, Tobias Borsdorff, Ilse Aben, Róisín

Commane, Bruce Daube, et al. 2020. “1.5 Years of TROPOMI CO Measurements:

Comparisons to MOPITT and ATom.” *Atmospheric Measurement Techniques* 13 (9): 4841–64. <https://doi.org/10.5194/amt-13-4841-2020>.

Martínez-Alonso, Sara, Merritt N. Deeter, Bianca C. Baier, Kathryn McKain, Helen Worden, Tobias Borsdorff, Colm Sweeney, and Ilse Aben. 2022. “Evaluation of MOPITT and TROPOMI Carbon Monoxide Retrievals Using AirCore in Situ Vertical Profiles.” *Atmospheric Measurement Techniques* 15 (16): 4751–65. <https://doi.org/10.5194/amt-15-4751-2022>.

Martínez-Alonso, Sara, Merritt N. Deeter, Helen M. Worden, John C. Gille, Louisa K. Emmons, Laura L. Pan, Mijeong Park, et al. 2014. “Comparison of Upper Tropospheric Carbon Monoxide from MOPITT, ACE-FTS, and HIPPO-QCLS.” *Journal of Geophysical Research: Atmospheres* 119 (24): 14,144–14,164. <https://doi.org/10.1002/2014JD022397>.

Masri, Shahir, Erica Scaduto, Yufang Jin, and Jun Wu. 2021. “Disproportionate Impacts of Wildfires among Elderly and Low-Income Communities in California from 2000–2020.” *International Journal of Environmental Research and Public Health* 18 (8): 3921. <https://doi.org/10.3390/ijerph18083921>.

Marvin, Margaret R., Paul I. Palmer, Fei Yao, Mohd Talib Latif, and Md Firoz Kahn. 2023. “Uncertainties from Biomass Burning Aerosols in Air Quality Models Obscure Public Health Impacts in Southeast Asia.” Preprint. *Aerosols/Atmospheric Modelling and Data Analysis/Troposphere/Chemistry (chemical composition and reactions)*. <https://doi.org/10.5194/egusphere-2023-1232>.

McClure, Crystal D., and Daniel A. Jaffe. 2018. "US Particulate Matter Air Quality Improves except in Wildfire-Prone Areas." *Proceedings of the National Academy of Sciences* 115 (31): 7901–6. <https://doi.org/10.1073/pnas.1804353115>.

Mettig, Nora, Mark Weber, Alexei Rozanov, John P. Burrows, Pepijn Veeffkind, Anne M. Thompson, Ryan M. Stauffer, et al. 2022. "Combined UV and IR Ozone Profile Retrieval from TROPOMI and CrIS Measurements." *Atmospheric Measurement Techniques* 15 (9): 2955–78. <https://doi.org/10.5194/amt-15-2955-2022>.

Migliaccio, Christopher T., Emily Kobos, Quinton O. King, Virginia Porter, Forrest Jessop, and Tony Ward. 2013. "Adverse Effects of Wood Smoke PM 2.5 Exposure on Macrophage Functions." *Inhalation Toxicology* 25 (2): 67–76. <https://doi.org/10.3109/08958378.2012.756086>.

National Interagency Fire Center. 2020. National Large Incident Year-to-Date Report. <https://web.archive.org/web/20201229021815/https://gacc.nifc.gov/sacc/predictive/intelligence/NationalLargeIncidentYTDRreport.pdf>.

Northwest Interagency Coordination Center. 2021. "Northwest Annual Fire Report 2020." Portland, OR. https://gacc.nifc.gov/nwcc/content/pdfs/archives/2020_NWCC_Annual_Fire_Report.pdf.

Olsen, Kevin S., Kimberly Strong, Kaley A. Walker, Chris D. Boone, Piera Raspollini, Johannes Plieninger, Whitney Bader, et al. 2017. "Comparison of the GOSAT TANSO-FTS TIR CH₄ Volume Mixing Ratio Vertical Profiles with Those

- Measured by ACE-FTS, ESA MIPAS, IMK-IAA MIPAS, and 16 NDACC Stations.”
Atmospheric Measurement Techniques 10 (10): 3697–3718. <https://doi.org/10.5194/amt-10-3697-2017>.
- Ortega, Ivan, Rebecca R. Buchholz, Emrys G. Hall, Dale F. Hurst, Allen F. Jordan, and James W. Hannigan. 2019. “Tropospheric Water Vapor Profiles Obtained with FTIR: Comparison with Balloon-Borne Frost Point Hygrometers and Influence on Trace Gas Retrievals.”
Atmospheric Measurement Techniques 12 (2): 873–90. <https://doi.org/10.5194/amt-12-873-2019>.
- Pfister, G. G., L. K. Emmons, P. G. Hess, J.-F. Lamarque, J. J. Orlando, S. Walters, A. Guenther, P. I. Palmer, and P. J. Lawrence. 2008. “Contribution of Isoprene to Chemical Budgets: A Model Tracer Study with the NCAR CTM MOZART-4: ISOPRENE IN MOZART-4.”
Journal of Geophysical Research: Atmospheres 113 (D5): n/a-n/a.
<https://doi.org/10.1029/2007JD008948>.
- Reid, Colleen E., Ellen M. Considine, Melissa M. Maestas, and Gina Li. 2021. “Daily PM_{2.5} Concentration Estimates by County, ZIP Code, and Census Tract in 11 Western States 2008–2018.” *Scientific Data* 8 (1): 112. <https://doi.org/10.1038/s41597-021-00891-1>.
- Reid, Colleen E., Michael Brauer, Fay H. Johnston, Michael Jerrett, John R. Balmes, and Catherine T. Elliott. 2016. “Critical Review of Health Impacts of Wildfire Smoke Exposure.” *Environmental Health Perspectives* 124 (9): 1334–43.
<https://doi.org/10.1289/ehp.1409277>.

- Reid, Colleen E., Michael Jerrett, Maya L. Petersen, Gabriele G. Pfister, Philip E. Morefield, Ira B. Tager, Sean M. Raffuse, and John R. Balmes. 2015. "Spatiotemporal Prediction of Fine Particulate Matter During the 2008 Northern California Wildfires Using Machine Learning." *Environmental Science & Technology* 49 (6): 3887–96.
<https://doi.org/10.1021/es505846r>.
- Reisen F, Duran SM, Flannigan M, Elliott C, Rideout K (2015) Wildfire smoke and public health risk. *International Journal of Wildland Fire* 24, 1029–1044. doi:10.1071/WF15034
- Rémy, Samuel, Andreas Veira, Ronan Paugam, Mikhail Sofiev, Johannes W. Kaiser, Franco Marengo, Sharon P. Burton, et al. 2017. "Two Global Data Sets of Daily Fire Emission Injection Heights since 2003." *Atmospheric Chemistry and Physics* 17 (4): 2921–42.
<https://doi.org/10.5194/acp-17-2921-2017>.
- Robeson, Scott M. 2015. "Revisiting the Recent California Drought as an Extreme Value." *Geophysical Research Letters* 42 (16): 6771–79. <https://doi.org/10.1002/2015GL064593>.
- Roces-Díaz, Jose V, Cristina Santín, Jordi Martínez-Vilalta, and Stefan H Doerr. 2022. "A Global Synthesis of Fire Effects on Ecosystem Services of Forests and Woodlands." *Frontiers in Ecology and the Environment* 20 (3): 170–78. <https://doi.org/10.1002/fee.2349>.
- Rodgers, C. D. 2000. *Inverse Methods for Atmospheric Sounding: Theory and Practice*, World Scientific. London.
- Rogers, R. R., and Man Kong Yau. 1989. *A Short Course in Cloud Physics*. 3rd ed. International Series in Natural Philosophy, v. 113. Oxford ; New York: Pergamon Press.

- Romero-Lankao, Vicente R., and Christopher B. Smith. 2014. "North America." In *Climate Change 2014: Impacts, Adaptation and Vulnerability*, edited by David Jon Dokken, Michael D. Mastrandrea, and Katharine J. Mach, 1439–98. Cambridge: Cambridge University Press. <https://doi.org/10.1017/CBO9781107415386.006>.
- Schneider, M., F. Hase, and T. Blumenstock. 2006. "Water Vapour Profiles by Ground-Based FTIR Spectroscopy: Study for an Optimised Retrieval and Its Validation." *Atmospheric Chemistry and Physics* 6 (3): 811–30. <https://doi.org/10.5194/acp-6-811-2006>.
- Seinfeld, John H, and Spyros N Pandis. 2016. *Atmospheric Chemistry and Physics: From Air Pollution to Climate Change*. John Wiley & Sons.
- Seinfeld, John H., and Spyros N. Pandis. 2012. *Atmospheric Chemistry and Physics: From Air Pollution to Climate Change*. 2. Aufl.;3rd; Book, Whole. Somerset: Wiley-Interscience. <https://go.exlibris.link/d1B7qbDR>.
- Sena E T, Artaxo P and Correia A L 2013 Spatial variability of the direct radiative forcing of biomass burning aerosols and the effects of land use change in Amazonia *Atmos. Chem. Phys.* 13 1261–75
- Sha, Mahesh Kumar, Bavo Langerock, Jean-François L. Blavier, Thomas Blumenstock, Tobias Borsdorff, Matthias Buschmann, Angelika Dehn, et al. 2021. "Validation of Methane and Carbon Monoxide from Sentinel-5 Precursor Using TCCON and NDACC-IRWG Stations." *Atmospheric Measurement Techniques* 14 (9): 6249–6304. <https://doi.org/10.5194/amt-14-6249-2021>.

Stephens, Scott L., Jan W. Van Wagtendonk, James K. Agee, and Ronald H. Wakimoto. 2021.

“Introduction to the Article by Harold Biswell: Prescribed Burning in Georgia and California Compared.” *Fire Ecology* 17 (1): 9. <https://doi.org/10.1186/s42408-021-00094-4>.

Sutherland, E. Rand, Barry J. Make, Sverre Vedal, Lening Zhang, Steven J. Dutton, James R.

Murphy, and Philip E. Silkoff. 2005. “Wildfire Smoke and Respiratory Symptoms in Patients with Chronic Obstructive Pulmonary Disease.” *Journal of Allergy and Clinical Immunology* 115 (2): 420–22. <https://doi.org/10.1016/j.jaci.2004.11.030>.

Tang, Wenfu, Louisa K. Emmons, Rebecca R. Buchholz, Christine Wiedinmyer, Rebecca H.

Schwantes, Cenlin He, Rajesh Kumar, et al. 2022. “Effects of Fire Diurnal Variation and Plume Rise on U.S. Air Quality During FIREX-AQ and WE-CAN Based on the Multi-Scale Infrastructure for Chemistry and Aerosols (MUSICAv0).” *Journal of Geophysical Research: Atmospheres* 127 (16): e2022JD036650.

<https://doi.org/10.1029/2022JD036650>.

Thangavel, Prakash, Duckshin Park, and Young-Chul Lee. 2022. “Recent Insights into

Particulate Matter (PM_{2.5})-Mediated Toxicity in Humans: An Overview.” *International Journal of Environmental Research and Public Health* 19 (12): 7511.

<https://doi.org/10.3390/ijerph19127511>.

Thapa, Laura H., Xinxin Ye, Johnathan W. Hair, Marta A. Fenn, Taylor Shingler, Shobha

Kondragunta, Charles Ichoku, et al. 2022. “Heat Flux Assumptions Contribute to

- Overestimation of Wildfire Smoke Injection into the Free Troposphere.” *Communications Earth & Environment* 3 (1): 236. <https://doi.org/10.1038/s43247-022-00563-x>.
- Vidot, J., J. Landgraf, O.P. Hasekamp, A. Butz, A. Galli, P. Tol, and I. Aben. 2012. “Carbon Monoxide from Shortwave Infrared Reflectance Measurements: A New Retrieval Approach for Clear Sky and Partially Cloudy Atmospheres.” *Remote Sensing of Environment* 120 (May): 255–66. <https://doi.org/10.1016/j.rse.2011.09.032>.
- Voulgarakis, Apostolos, and Robert D. Field. 2015. “Fire Influences on Atmospheric Composition, Air Quality and Climate.” *Current Pollution Reports* 1 (2): 70–81. <https://doi.org/10.1007/s40726-015-0007-z>.
- Ward D S, Kloster S, Mahowald N M, Rogers B M, Randerson J T and Hess P G 2012 The changing radiative forcing of fires: global model estimates for past, present and future *Atmos. Chem. Phys.* 12 10857–86
- Wegesser TC, Pinkerton KE, Last JA (2009) California wildfires of 2008: coarse and fine particulate matter toxicity. *Environmental Health Perspectives* 117, 893–897. doi:10.1289/EHP.0800166
- Wegesser, Teresa C., Kent E. Pinkerton, and Jerold A. Last. 2009. “California Wildfires of 2008: Coarse and Fine Particulate Matter Toxicity.” *Environmental Health Perspectives* 117 (6): 893–97. <https://doi.org/10.1289/ehp.0800166>.
- Wennberg, P. O., C.M. Roehl, D Wunch, J.-F. Blavier, G. C. Toon, N. T. Allen, R. Treffers, and J. Laughner. 2023. “TCCON Data from Caltech (US), Release GGG2020.R0.” CaltechDATA. <https://doi.org/10.14291/TCCON.GGG2020.PASADENA01.R0>.

- Wilkins, Joseph L., George Pouliot, Kristen Foley, Wyatt Appel, and Thomas Pierce. 2018. “The Impact of US Wildland Fires on Ozone and Particulate Matter: A Comparison of Measurements and CMAQ Model Predictions from 2008 to 2012.” *International Journal of Wildland Fire* 27 (10): 684. <https://doi.org/10.1071/WF18053>.
- Wolfe, Robert E., Guoqing Lin, Masahiro Nishihama, Krishna P. Tewari, James C. Tilton, and Alice R. Isaacman. 2013. “Suomi NPP VIIRS Prelaunch and On-orbit Geometric Calibration and Characterization.” *Journal of Geophysical Research: Atmospheres* 118 (20). <https://doi.org/10.1002/jgrd.50873>.
- Worden, H. M., J. A. Logan, J. R. Worden, R. Beer, K. Bowman, S. A. Clough, A. Eldering, et al. 2007. “Comparisons of Tropospheric Emission Spectrometer (TES) Ozone Profiles to Ozonesondes: Methods and Initial Results.” *Journal of Geophysical Research* 112 (D3): D03309. <https://doi.org/10.1029/2006JD007258>.
- Worden, H. M., M. N. Deeter, C. Frankenberg, M. George, F. Nichitiu, J. Worden, I. Aben, et al. 2013. “Decadal Record of Satellite Carbon Monoxide Observations.” *Atmospheric Chemistry and Physics* 13 (2): 837–50. <https://doi.org/10.5194/acp-13-837-2013>.
- Worden, J. R., A. J. Turner, A. Bloom, S. S. Kulawik, J. Liu, M. Lee, R. Weidner, et al. 2015. “Quantifying Lower Tropospheric Methane Concentrations Using GOSAT Near-IR and TES Thermal IR Measurements.” *Atmospheric Measurement Techniques* 8 (8): 3433–45. <https://doi.org/10.5194/amt-8-3433-2015>.
- Wunch, Debra, Geoffrey C. Toon, Jean-François L. Blavier, Rebecca A. Washenfelder, Justus Notholt, Brian J. Connor, David W. T. Griffith, Vanessa Sherlock, and Paul O. Wennberg.

2011. “The Total Carbon Column Observing Network.” *Philosophical Transactions of the Royal Society A: Mathematical, Physical and Engineering Sciences* 369 (1943): 2087–2112. <https://doi.org/10.1098/rsta.2010.0240>.
- Yang, Yang, Minqiang Zhou, Bavo Langerock, Mahesh Kumar Sha, Christian Hermans, Ting Wang, Denghui Ji, et al. 2020. “New Ground-Based Fourier-Transform near-Infrared Solar Absorption Measurements of XCO₂, XCH₄ and XCO at Xianghe, China.” *Earth System Science Data* 12 (3): 1679–96. <https://doi.org/10.5194/essd-12-1679-2020>.
- Ye, Xinxin, Mina Deshler, Alexi Lyapustin, Yujie Wang, Shobha Kondragunta, and Pablo Saide. 2022. “Assessment of Satellite AOD during the 2020 Wildfire Season in the Western U.S.” *Remote Sensing* 14 (23): 6113. <https://doi.org/10.3390/rs14236113>.
- Ye, Xinxin, Mina Deshler, Alexi Lyapustin, Yujie Wang, Shobha Kondragunta, and Pablo Saide. 2022. “Assessment of Satellite AOD during the 2020 Wildfire Season in the Western U.S.” *Remote Sensing* 14 (23): 6113. <https://doi.org/10.3390/rs14236113>.
- Ye, Xinxin, Pargoal Arab, Ravan Ahmadov, Eric James, Georg A. Grell, Bradley Pierce, Aditya Kumar, et al. 2021. “Evaluation and Intercomparison of Wildfire Smoke Forecasts from Multiple Modeling Systems for the 2019 Williams Flats Fire.” *Atmospheric Chemistry and Physics* 21 (18): 14427–69. <https://doi.org/10.5194/acp-21-14427-2021>.
- Youssef H, Liousse C, Roblou L, Assamoi EM, Salonon RO, Maesano C, Banerjee S, Annesi-Maesano I (2014) Non-Accidental Health Impacts of Wildfire Smoke. *International*

Journal of Environmental Research and Public Health 11, 11772–11804.

doi:10.3390/IJERPH111111772

Youssef, Hassani, Catherine Liousse, Laurent Roblou, Eric-Michel Assamoi, Raimo Salonen, Cara Maesano, Soutrik Banerjee, and Isabella Annesi-Maesano. 2014. “Non-Accidental Health Impacts of Wildfire Smoke.” *International Journal of Environmental Research and Public Health* 11 (11): 11772–804. <https://doi.org/10.3390/ijerph111111772>.

Zhang, Huanxin, Jun Wang, Lorena Castro García, Cui Ge, Todd Plessel, James Szykman, Benjamin Murphy, and Tanya L. Spero. 2020. “Improving Surface PM 2.5 Forecasts in the United States Using an Ensemble of Chemical Transport Model Outputs: 1. Bias Correction With Surface Observations in Nonrural Areas.” *Journal of Geophysical Research: Atmospheres* 125 (14). <https://doi.org/10.1029/2019JD032293>.

Zhang, Yiwen, Tingting Ye, Pei Yu, Rongbin Xu, Gongbo Chen, Wenhua Yu, Jiangning Song, Yuming Guo, and Shanshan Li. 2023. “Preterm Birth and Term Low Birth Weight Associated with Wildfire-Specific PM_{2.5}: A Cohort Study in New South Wales, Australia during 2016–2019.” *Environment International* 174 (April): 107879. <https://doi.org/10.1016/j.envint.2023.107879>.

Zhou, Xiaodan, Kevin Josey, Leila Kamareddine, Miah C. Caine, Tianjia Liu, Loretta J. Mickley, Matthew Cooper, and Francesca Dominici. 2021. “Excess of COVID-19 Cases and Deaths Due to Fine Particulate Matter Exposure during the 2020 Wildfires in the United States.” *Science Advances* 7 (33): eabi8789. <https://doi.org/10.1126/sciadv.abi8789>.